Biallelic variants in *ASNA1*, encoding a cytosolic targeting factor of tail-anchored proteins, cause rapidly progressive pediatric cardiomyopathy

Judith M.A. Verhagen, Myrthe van den Born, Herma C. van der Linde, Peter G.J. Nikkels, Rob M. Verdijk, Maryann H. Kivlen, Leontine M.A. van Unen, Annette F. Baas, MD, Henriette ter Heide, Lennie van Osch-Gevers, Marianne Hoogeveen-Westerveld, Johanna C. Herkert, Aida M. Bertoli-Avella, Marjon A. van Slegtenhorst, Marja W. Wessels, Frans W. Verheijen, David Hassel, Robert M.W. Hofstra, Ramanujan S. Hegde, Peter M. van Hasselt*, Tjakko J. van Ham*, Ingrid M.B.H. van de Laar*

**These authors contributed equally*

Manuscript submitted

Supplemental Videos are available online

Abstract

Background

Pediatric cardiomyopathies are a clinically and genetically heterogeneous group of heart muscle disorders associated with high morbidity and mortality. Although knowledge of the genetic basis of pediatric cardiomyopathy has improved considerably, the underlying cause remains elusive in a substantial proportion of cases.

Methods

Exome sequencing was used to screen for the causative genetic defect in a pair of siblings with rapidly progressive dilated cardiomyopathy and death in early infancy. Protein expression was assessed in patient samples, followed by an *in vitro* tail-anchored protein insertion assay and functional analyses in zebrafish.

Results

We identified compound heterozygous variants in the highly conserved *ASNA1* gene, which encodes an ATPase required for post-translational membrane insertion of tail-anchored proteins. The c.913C>T variant on the paternal allele is predicted to result in a premature stop codon p.(Gln305*), and likely explains the decreased protein expression observed in myocardial tissue and skin fibroblasts. The second variant, c.867C>G p.(Cys289Trp), leads to protein misfolding as well as less effective tail-anchored protein insertion. Loss of *asna1* in zebrafish resulted in reduced cardiac contractility and early lethality. In contrast to wild-type mRNA, injection of either mutant mRNA failed to rescue this phenotype.

Conclusions

Biallelic variants in *ASNA1* cause severe pediatric cardiomyopathy and early death. Our findings point toward a critical role of the tail-anchored membrane protein insertion pathway in vertebrate cardiac function and disease.

Introduction

Dilated cardiomyopathy (DCM) is defined by otherwise unexplained ventricular dilatation and impaired systolic function, that can result in progressive heart failure, arrhythmias and premature death [1]. To date, disease-causing variants in over 30 genes have been reported in DCM; the majority encoding structural proteins of cardiomyocytes such as titin (*TTN*), lamin A/C (*LMNA*) and myosin heavy chain 7 (*MYH7*) [2]. The same genes that are involved in adult-onset DCM also contribute to pediatric DCM, although the exact frequencies are unclear [3, 4]. *De novo* variants or a combination of multiple inherited variants may explain early-onset and/or severe disease presentation [3, 5]. Pediatric DCM can also be part of numerous syndromes, and neuromuscular or metabolic disorders. However, the underlying cause remains unknown in approximately 50% of cases [6, 7].

Here, we used family-based exome sequencing and subsequent functional validation to identify compound heterozygous variants in *ASNA1* in two siblings with early infantile-onset, rapidly progressive DCM. ASNA1, also known as TRC40 or GET3, is a ubiquitously expressed cytosolic chaperone that mediates insertion of tail-anchored (TA) proteins into the endoplasmic reticulum (ER) membrane [8]. TA proteins are membrane proteins characterized by a single hydrophobic transmembrane domain near the C-terminus which serves as both a targeting signal and a membrane anchor [9]. TA proteins constitute approximately 5% of integral membrane proteins and are involved in a variety of cellular processes, such as protein translocation, vesicle trafficking, and apoptosis [10]. Previous animal studies have implicated ASNA1-mediated membrane insertion of TA proteins in early embryonic development [11-16]. This study offers the first evidence for its role in human disease, and provides new insight into the molecular mechanisms in DCM.

Methods

Study participants

Affected individuals were recruited from the three clinical genetic centers in the Netherlands. All samples were collected after obtaining informed consent in compliance with clinical research protocols approved by the local institutional review boards.

Clinical evaluation

The diagnosis of DCM was made based on current practice guidelines [1, 17] Biochemical analysis in both affected siblings included quantitative analysis of lactate, amino acids, organic acids, carnitine and acylcarnitines, oligosaccharides, and isoelectric focusing of transferrin

and apolipoprotein C-III. Family members who participated in this study underwent cardiac screening with electrocardiogram and echocardiography.

Exome sequencing

Genomic DNA was extracted from peripheral blood samples using standard protocols, and fragmented by sonication. Exons were captured using the SureSelect Human All Exon V4 (Agilent Technologies). Sequencing was performed on a Hiseq 2000 system (Illumina) for 101 base pair paired-end runs. Reads were mapped to the human reference genome GRCh37/hg19 using the Burrows-Wheeler Aligner (BWA) [18]. Variants were called using the Genome Analysis Toolkit (GATK) [19], and filtered using Cartagenia Bench Lab software. We selected for rare variants (minor allele frequency <0.1% in public variant databases), focusing only on exonic and splice site variants. Apparent *de novo*, homozygous and compound heterozygous variants were considered for further analysis.

Sanger sequencing

Bidirectional Sanger sequencing of the entire coding region and exon-intron boundaries of the candidate genes was performed using PCR primers designed by Primer3 software (**Supplemental Table 1**). PCR products were purified and subsequently sequenced using the BigDye Terminator v3.1 kit on an ABI 3730xl DNA Analyzer (Life Technologies). Sequence data was analyzed using SeqScape v2.5 software. For annotation of DNA and protein changes, the mutation nomenclature recommendations from the Human Genome Variation Society were followed. To describe variants at the cDNA level, the A of the translation initiation codon of the reference sequence was designated as position +1.

Histology and immunostaining

Paraffin-embedded, hematoxylin and eosin (H&E) stained myocardial tissue from both affected siblings was examined using standard techniques. For immunohistochemistry, sections were deparaffinized and rehydrated before antibody retrieval. Primary antibodies included: full-length rabbit polyclonal anti-TRC40 (non-commercial, dilution 1:400) [8], mouse monoclonal anti-N-cadherin (Agilent Technologies #M3616, dilution 1:200), and mouse monoclonal anti-desmin (Ventana Medical Systems #760-2513, prediluted). The slides were counterstained with hematoxylin II for 8 minutes and bluing reagent for 8 minutes according to the manufacturer's instructions (Ventana Medical Systems). Immunostained preparations were analyzed by light microscopy. Glutaraldehyde-fixed myocardial tissue was prepared for electron microscopy. Immunolabeling was performed on cryosections as described previously [20]. Primary antibodies included: mouse monoclonal anti-N-cadherin (Sigma-Aldrich #C3865, 1:800) and mouse monoclonal anti-emerin (Novocastra Laboratories #NCL-EMERIN). Secondary labeling was performed with appropriate Texas Red (N-cadherin) or fluorescein isothiocyanate–conjugated antibodies (emerin). After immunolabeling, sections

were analysed with a Nikon Eclipse 80i epifluorescence microscope, and images were taken using a DS-2BWc digital sight camera and NIS-Elements BR 3.0 software (Nikon Instruments).

Western blotting

Cultured skin fibroblasts from one patient (individual II:2) and three control individuals were lysed in 100 µL TNE buffer [50 mM Tris-HCl (pH 7.6), 100 mM NaCl, 50 mM NaF, 1% (v/v) Triton X-100] and cOmplete Protease Inhibitor Cocktail tablets (Roche Applied Science). Lysates were centrifuged for 10 minutes at 10,000 rpm to remove small cell debris. Equal amounts (20 µg or 40 µg) of protein were separated on a 4-15% precast polyacrylamide gel (Bio-Rad Laboratories). Rabbit polyclonal antibodies against the full-length (non-commercial; dilution 1:2000) and N-terminus (non-commercial; dilution 1:2000) of human ASNA1 were used for detection [8]. Results were normalized to the GAPDH loading control.

In vitro synthesis of mRNA

Total RNA was extracted from human skin fibroblasts using the RNeasy Mini Kit (QIAGEN), and converted into cDNA using the iScript Reverse Transcription Supermix (Bio-Rad Laboratories, #1708840). Products were ligated into the pCMV6-entry vector with C-terminal Myc-DDK tag, and subsequently transformed into XL10-Gold ultracompetent cells (Stratagene). All constructs were verified by DNA sequencing. Expression of recombinant proteins was checked after transfection into human embryonic kidney (HEK) 293 cells using previously described rabbit polyclonal antibodies raised against the full-length and N-terminal peptide of human ASNA1 [8]. Linearized constructs were used as a template for *in vitro* synthesis of capped mRNA using the mMESSAGE mMACHINE T7 Transcription Kit (Thermo Fisher Scientific).

Purification of recombinant ASNA1

The construct for wild-type zebrafish ASNA1 (TRC40) expression in *E. coli* has been described previously [21]. It contains an N-terminal 6xHis tag and tobacco etch virus (TEV) protease cleavage site, followed by the full-length ASNA1 open reading frame. The Val163Ala variant was introduced into this construct by site-directed mutagenesis and verified by sequencing. Expression and purification from *E. coli* used minor modifications of previously published methods (see Detailed Methods, **Supplemental Information**) [21, 22].

Analysis of ASNA1 protein function in vitro

Thermal stability of the purified wild-type and Val163Ala mutant ASNA1 protein was analyzed using the Prometheus NT.48 system (NanoTemper Technologies). Purified protein at 0.8 mg/mL was monitored for intrinsic tryptophan fluorescence during a temperature ramp from 20°C to 95°C. A change in the ratio of emission at 330 nm and 350 nm was used to measure unfolding. The ability of ASNA1 protein to capture TA protein was assayed exactly as described previously (see Detailed Methods, **Supplemental Information**) [21].

Phenotypic analysis of mutant zebrafish

Zebrafish *asna1* (ENSDARG00000018190) was targeted by Cas9/gRNA complex injection as described previously [23]. Further specifications are provided in the **Supplemental Information**, **Supplemental Table 2** and **Supplemental Figure 1**. Zebrafish were anesthetized with tricaine methanesulfonate (MS-222) and imaged using a Leica M165 FC stereo microscope connected to a Leica DFC550 digital camera. Zebrafish were positioned horizontally in 5% methylcellulose to obtain a lateral view of the ventricle. Heart rate (beats/minute) was calculated by three independent counts of the number of beats in 15 second intervals. Fractional shortening (%) was derived from linear measurements of the ventricle at end-diastole and end-systole [24]. Blood flow rate was determined by visual inspection and classified as "normal", "decreased" or "absent". For microscopic analysis, zebrafish larvae (n=4 for each group) were anesthetized, fixed in Karnovsky fixative (PBS containing 2% paraformaldehyde and 3% glutaraldehyde), and embedded in Epon. Semithin sections (1 µm) were stained with toluidine blue and studied under a light microscope. Ultrathin sections (70 nm) were stained with 5% uranyl acetate and 2.5% lead citrate, and photographically recorded using a JEOL 1200-EX II transmission electron microscope.

Bioinformatics

In order to find proteins that might be affected by defective ASNA1-mediated membrane insertion, we obtained a list of all human single-pass membrane proteins from UniProt [25]. We first removed all proteins that contain an N-terminal signal sequence, and from the remainder, selected for proteins that contain a transmembrane domain within the last 50 residues from the C-terminus. The final list contained 286 predicted human TA proteins (**Supplemental Table 3**). We investigated the potential association between the corresponding genes and cardiomyopathy using the Online Mendelian Inheritance in Man database (https://www.omim.org).

Statistical analysis

Statistical analyses were performed using Microsoft Excel or GraphPad Prism software. Continuous variables were expressed as means ± standard deviation, and compared using the Student's t-test. Categorical variables were expressed as counts and percentages, and compared using the Fisher's exact test. An asterisk (*) indicates p-values lower than 0.05.

Results

Clinical presentation

The proband (**Figure 1A**: II:2) was the second child of non-consanguineous Caucasian parents, born at term after an uneventful pregnancy. At age 2 weeks, she presented with severe

tachypnea and feeding difficulties. No dysmorphic features were observed. Echocardiography revealed a small muscular ventricular septal defect (VSD), an ostium secundum atrial septal defect, and impaired left ventricular (LV) contractility (LV ejection fraction 41%) (**Figure 2A and 2B**, **Supplemental Figure 2A**). ECG recordings showed sinus rhythm with broad QRS complexes (**Supplemental Figure 3A**). After rapid clinical deterioration with brief circulatory arrest, she was transferred to a tertiary referral hospital for extracorporeal membrane oxygenation. LV function remained poor without any signs of improvement. In addition, a large LV thrombus developed refractory to medical therapy (**Supplemental Video 1**). The patient died at age 7 weeks.

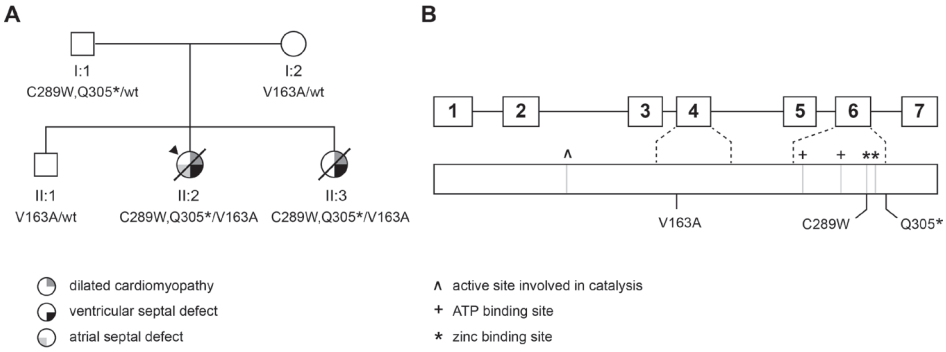

C

Human *(Homo sapiens)*	RLVKGMNFSV**V**VFDTAPTGHT	PEKP**C**KMCEARHKIQAKYLD**Q**
Mouse *(Mus musculus)*	RLVKGMNFSV**V**VFDTAPTGHT	PEKP**C**KMCEARHKIQAKYLD**Q**
Dog *(Canis lupus familiaris)*	RLVKGINFSV**V**VFDTAPTGHT	PKKP**C**KMCEAHHKIQAKYLD**Q**
Frog *(Xenopus familiaris)*	RLVKGMNFSV**V**VFDTAPTGHT	PENRFSMCESRLMMQSKYVGH
Zebrafish *(Danio rerio)*	RLVKGMNFSV**V**VFDTAPTGHT	NERP**C**KMCEARHKIQSKYLD**Q**
Fruitfly *(Drosophila melanogaster)*	KLVKGMNFSV**V**VFDTAPTGHT	SHDS**C**SMCASRFKIQEKYLD**Q**
Roundworm *(Caenorhabditis elegans)*	ELIDSLGFDV**V**VFDTAPTGHT	ENGAVSRRKCAQQTQASTSDP
Yeast *(Saccharomyces cerevisiae)*	KHIKGETFDT**V**IFDTAPTGHT	QEHN**C**KRCQARWKMQKKYLD**Q**

Figure 1. (A) Pedigree of the family. Squares and circles indicate males and females, respectively. The arrowhead indicates the proband. Upper right symbols indicate dilated cardiomyopathy, lower right symbols indicate ventricular septal defect, and lower left symbol indicates atrial septal defect. Genetic status is displayed below the symbols: wt, wild-type. (B) Schematic overview of the *ASNA1* gene (top) and corresponding protein (bottom). Boxes represent exons; connecting lines represent intervening introns. ^ indicates active site involved in catalysis, + indicates ATP binding sites, and * indicates zinc binding sites. Rare variants identified in our family are displayed at the bottom of the diagram. (C) Ortholog alignment of ASNA1 (derived from Ensembl reference sequences), showing high degree of protein conservation across vertebrates. Positions of disease-causing variants discovered in our family are indicated in bold.

Her younger sister (II:3) was born at term after an uneventful pregnancy with normal second-trimester advanced ultrasound examination. Because of the family history, echocardiography was performed at the first day postpartum showing a small midmuscular VSD but otherwise normal size and function of the heart (**Figure 2C**, **Supplemental Figure 2B**). She was re-examined after a week because of tachypnea. Echocardiographic findings were essentially unchanged (**Supplemental Video 2**). However, only three days later (age 12 days), she presented

with cardiorespiratory failure necessitating resuscitation. Echocardiography now showed dilatation of the heart chambers with poor contractility (**Figure 2D** and **Supplemental Video 3**). ECG recordings in the resuscitation setting were severely abnormal (**Supplemental Figure 3B**). The resuscitation attempt was terminated after 20 minutes.

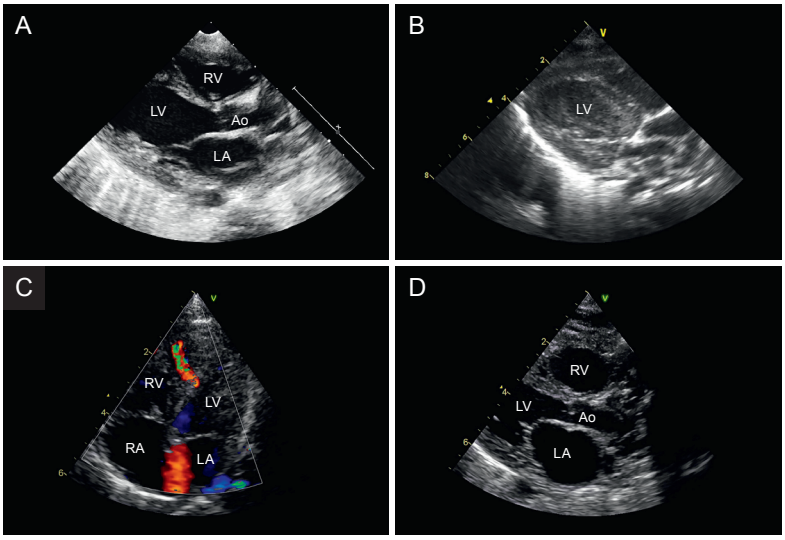

Figure 2. Cardiac ultrasound examination. Patient II:2 (A) Parasternal long-axis view during extracorporeal membrane oxygenation showing mild dilatation of the left ventricle; (B) intracardiac thrombus formation. Patient II:3 (C) Four-chamber view at first day postpartum showing a midmuscular ventricular septal defect. (D) Parasternal long-axis view during cardiopulmonary resuscitation showing dilatation of the heart chambers. Ao indicates aorta; LA, left atrium; LV, left ventricle; RA, right atrium; and RV, right atrium.

In both siblings, extensive biochemical, hematological, viral and metabolic testing was unremarkable except for slightly abnormal serum transferrin and apolipoprotein C-III isoelectric focusing profiles, indicative of a combined defect in N-linked and O-linked glycosylation. Cardiac screening in both parents (aged 36 and 37 years) and the elder brother (aged 34 months) revealed no abnormalities.

Exome sequencing

Targeted next-generation sequencing (NGS) of 48 genes implicated in cardiomyopathy revealed no potentially deleterious variants [26]. Exome sequencing in the affected proband (II:2) and her healthy parents identified three novel heterozygous variants in *ASNA1* (NM_004317.2): two variants c.867C>G p.(Cys289Trp) and c.913C>T p.(Gln305*) in *cis* configuration on the paternal allele, and a missense variant c.488T>C p.(Val163Ala) on the maternal allele (**Figure 1A and 1B**). No other potentially deleterious variants were detected. We confirmed that the affected sister (II:3) carried all three *ASNA1* variants. The unaffected brother (II:1) had inherited only the maternally derived *ASNA1* variant (**Figure 1A**). All variants were absent from public

databases, including the nearly 140,000 alleles in gnomAD v2.0.2. The high pLI score (0.92) indicates that *ASNA1* is extremely intolerant to loss-of-function variants. Both missense variants were predicted to be deleterious (CADD>20 and M-CAP>0.025). The c.913C>T variant introduces a premature stop codon, likely resulting in the loss of the last 42 amino acids. In silico analysis did not predict an effect on splicing using the nearby splice site. Indeed, RT-PCR analysis showed no alternatively spliced transcripts (data not shown).

Cohort screening

In order to find additional cases, we sequenced 70 children with idiopathic cardiomyopathy for *ASNA1* variants using either Sanger sequencing or filtering of exome sequencing data. No biallelic variants were found. In one patient, presenting with severe DCM requiring heart transplantation at age 16 years, we identified one paternally inherited, heterozygous missense variant c.547G>A p.(Val183Met) in *ASNA1*. Genome-wide microarray analysis excluded a large deletion of the second allele. However, in addition, a *de novo* disease-causing variant c.473T>C p.(Leu158Pro) was found in *LMNA* (NM_17070.2), generally associated with adult-onset DCM. Although the *ASNA1* variant is rare and assigned to the top 1% most deleterious substitutions possible in the human genome (CADD score 23.1), it is predicted to be tolerated by SIFT and PolyPhen-2, and classified as likely benign by M-CAP. Nevertheless, given the relatively early onset and severe disease presentation, it cannot be excluded that this *ASNA1* variant acted as a modifier of the *LMNA*-related cardiomyopathy. A second search aiming to identify further patients was performed in Centogene's internal database, which contains NGS data from a heterogeneous cohort of 19,144 index patients with suspected genetic diseases and a total of 33,762 samples (as per July 2018). However, no additional patients were identified with rare biallelic variants in *ASNA1*.

Histopathologic examination

In both siblings, postmortem examination revealed an increased heart weight to body size and severe dilatation of the left ventricle (**Figure 3A**). Microscopic examination of the myocardium showed prominent subendothelial fibrosis. In age-matched controls, ASNA1 was predominantly localized to the cytoplasm and intercalated discs. Expression of ASNA1 was reduced in both patients compared to controls (**Figure 3B**). As demonstrated by N-cadherin labeling (**Figure 3B**) and electron microscopy (**Figure 3C**), in both patients, intercalated discs were irregular in appearance and intercellular space was increased. Desmin staining confirmed myofibrillar disorganization (**Figure 3B**). We examined the subcellular localization of the TA protein emerin in myocardium using immunofluorescence staining. Emerin correctly localized to the nuclear membrane. However, nuclei had an irregular shape (**Figure 3D**). Microscopic examination of other visceral organs did not reveal any obvious abnormalities (data not shown).

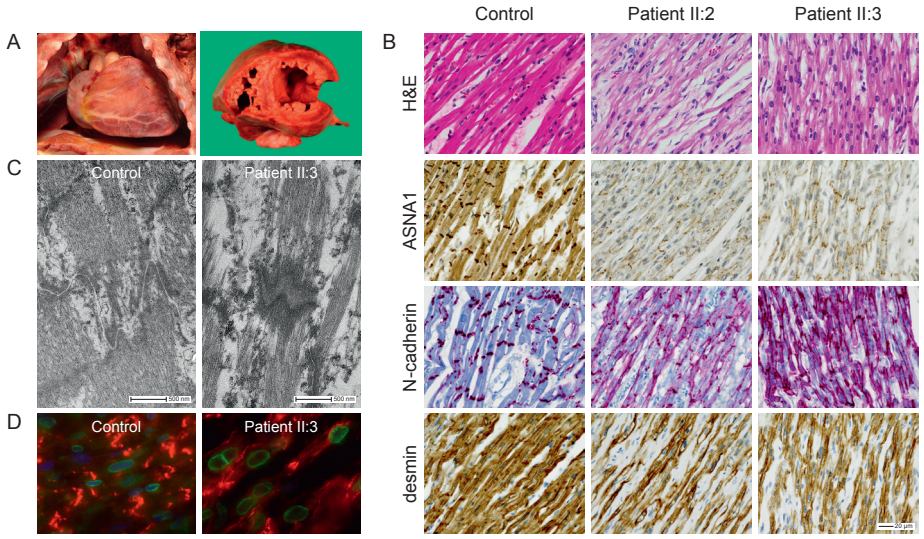

Figure 3. Histopathological features of the myocardium. (A) Macroscopic images showing an enlarged heart with dilated left ventricle in patient II:3. (B) Representative images of histological and immunohistochemical studies of myocardial tissue showing markedly reduced expression of ASNA1 at the cytoplasm and intercalated discs in both patients compared with an age-matched control. N-cadherin staining showing irregular appearance of the intercalated discs. Desmin staining showing myofibrillar disorganization. Scale bar: 20μm. (C) Electron microscope images of cardiac intercalated discs, showing increased intercellular space in the patient compared to an age-matched control. (D) Representative images of immunofluorescence double staining of emerin (nuclear membrane, green fluorescence) and N-cadherin (intercalated disc, red fluorescence) in myocardial tissue of patient and control. Note irregular nuclear shape in the patient.

Biochemical analysis of ASNA1 protein

As expected from the reduced ASNA1 expression by immunohistochemistry (**Figure 3B**), Western blot experiments confirmed that ASNA1 was decreased in fibroblasts of patient II:2 (**Figure 4A**), suggesting that mutant ASNA1 protein in this patient is unstable. This is to be expected for the (Cys289Trp;Gln305*) double mutant. The Cys289 variant is part of an essential zinc binding site; residues downstream of Gln305 would be essential for structural integrity of ASNA1 [22]. The other mutated residue, Val163, is universally conserved from yeast Get3 to human ASNA1 and forms part of the hydrophobic domain [22], suggesting that substitution of this residue might also lead to reduced stability and/or function of the protein. To explore this possibility, we investigated the consequences of the Val163Ala variant *in vitro* using recombinant zebrafish ASNA1 protein.

Although Val163Ala mutant ASNA1 was expressed equally well as wild-type ASNA1 in *E. coli*, the mutant was mostly insoluble indicating its inefficient folding (**Supplemental Figure 4A**). The folded population of mutant ASNA1 was purified (**Supplemental Figure 4B**) and shown to display comparable thermal stability as wild-type ASNA1 (**Figure 4B**). Recombinant mutant ASNA1 was also comparably efficient as wild-type ASNA1 in capturing a TA protein

substrate (**Figure 4C**) using a previously established *in vitro* assay [21]. However, TA protein in complex with mutant ASNA1 was very poorly inserted into ER microsomes compared to TA protein in complex with wild-type ASNA1 (**Figure 4D**). Thus, the Val163Ala variant has two consequences. First, it reduces the production of folded ASNA1 due to aggregation. Second, properly folded mutant ASNA1, while competent for TA protein interaction, is inefficient in facilitating TA protein insertion into the ER membrane.

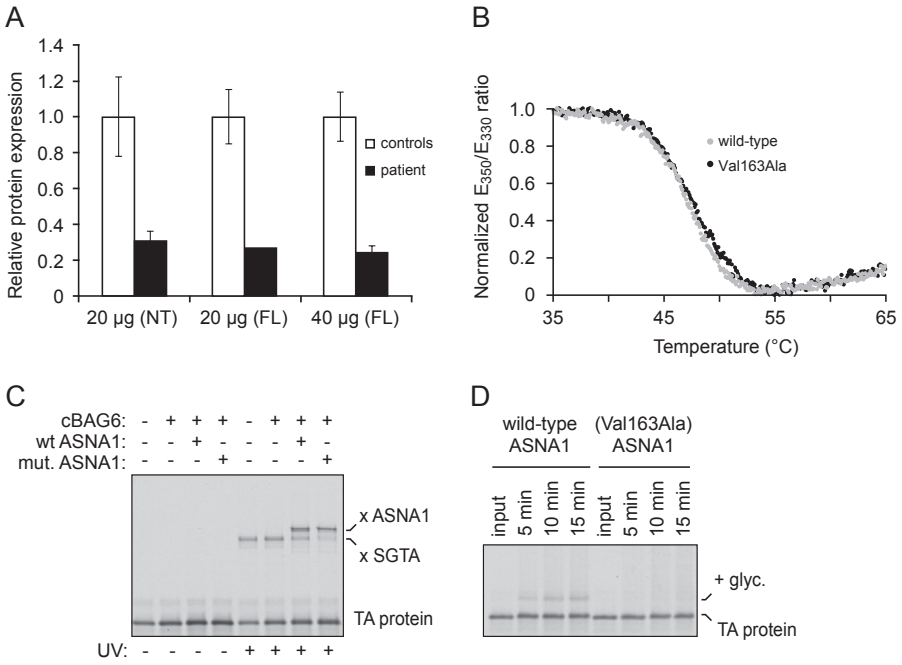

Figure 4. Biochemical analyses of ASNA1. (A) Expression levels of ASNA1 protein in skin fibroblasts from patient II:2 compared to healthy controls, and normalized against GAPDH as measured by Western blot analysis. Relative expression is expressed as mean ± standard deviation (SD) from 1-3 different experiments. Error bars represent SD. FL, full-length; NT, N-terminus. (B) Thermal unfolding curves of purified recombinant wild-type and Val163Ala mutant ASNA1. The ratio of tryptophan fluorescence emission at 350 nm to 330 nm was measured during a temperature ramp. The ratio was normalized using the highest and lowest values and scaled to 1.0 and 0, respectively. This ratio is sensitive to the environment around the tryptophan, and therefore changes during protein unfolding. Both wild-type and mutant ASNA1 unfold at the same temperature (between 45°C and 50°C), indicating that they are comparably stable. (C) Radiolabeled TA protein assembled on the chaperone SGTA was mixed with wild-type or mutant ASNA1 together with the cBAG6 complex (which bridges SGTA and ASNA1), incubated for 90 seconds, and subjected to UV-induced crosslinking. In the reaction lacking ASNA1, the TA protein crosslinks to SGTA (x SGTA) in a UV-dependent manner. Transfer from SGTA to ASNA1 (as evidenced by crosslinking to ASNA1 after incubation) is observed for wild-type and Val163Ala mutant ASNA1. (D) Radiolabeled TA protein in complex with either wild-type or Val163Ala mutant ASNA1 (Supplemental Figure 4D) was incubated with ER microsomes for the indicated times. "Input" indicates an aliquot of the starting complex analysed for comparison. ER insertion was monitored by the appearance of a glycosylated form of the TA protein (indicated by "+ glyc"). Insertion is less efficient for the reactions containing mutant ASNA1.

Zebrafish mutants

The zebrafish ortholog *asna1* shares 82% nucleotide identity with the human sequence. To confirm the role of *ASNA1* variants in cardiac disease, we generated *asna1*-deficient mutant zebrafish by CRISPR/Cas9-mediated genome editing. Incrossed heterozygous *asna1* mutants (*asna1*$^{\Delta 7/+}$) resulted in Mendelian ratios of progeny. On gross examination, *asna1*$^{\Delta 7/\Delta 7}$ embryos had impaired swim bladder inflation and smaller body size compared to their wild-type and heterozygous clutchmates (**Figure 5A**). From 5 dpf, *asna1*$^{\Delta 7/\Delta 7}$ mutants displayed abnormal cardiac contractions and decreased blood flow velocity in the dorsal aorta and cardinal vein (**Supplemental Video 4 and 5**). Fractional shortening was significantly reduced in *asna1*$^{\Delta 7/\Delta 7}$ mutants compared to wild-type and heterozygous clutchmates (p<0.05). Mean heart rate was not significantly different between all groups, even after cessation of blood flow (**Figure 5B**), pointing towards a primary defect in cardiac contractility and not the electrical system. Compatible with the findings in our family, heterozygous mutants (*asna1*$^{\Delta 7/+}$) did not show any overt phenotype. In contrast, none of the homozygous mutants (*asna1*$^{\Delta 7/\Delta 7}$) survived past 8 dpf.

On microscopic examination, hearts of *asna1*$^{\Delta 7/\Delta 7}$ zebrafish were irregular in shape and had thinner walls compared to wild-type and heterozygous clutchmates. In addition, electron microscopic examination revealed less organized Z-lines (plate-like structures that anchor actin filaments) and irregular intercalated discs in *asna1*$^{\Delta 7/\Delta 7}$ zebrafish (**Figure 5C** and **Supplemental Figure 4**). Injection of wild-type human *ASNA1* mRNA into *asna1*$^{\Delta 7/\Delta 7}$ zebrafish embryos significantly rescued the phenotype at each time point examined (p<0.0005) (**Figure 5D**). This rescue effect seems to disappear over time, likely due to mRNA degradation. In contrast to rescue observed with wild-type *ASNA1* mRNA, injection of either the paternal or maternal mutant *ASNA1* mRNA failed to rescue the disease phenotype (**Figure 5D**), supporting their pathogenicity.

Key candidate proteins

Inspection of the list of predicted human TA proteins (**Supplemental Table 3**) revealed seven proteins of interest that have been associated with cardiomyopathy in humans: myotonin-protein kinase (DMPK; Q09013), dysferlin (DYSF; O75923), emerin (EMD; P50402), junctophilin-2 (JPH2; Q9BR39), cardiac phospholamban (PPLA; P26678), nesprin-1 (SYNE1; Q8NF91) and nesprin-2 (SYNE2; Q8WXH0).

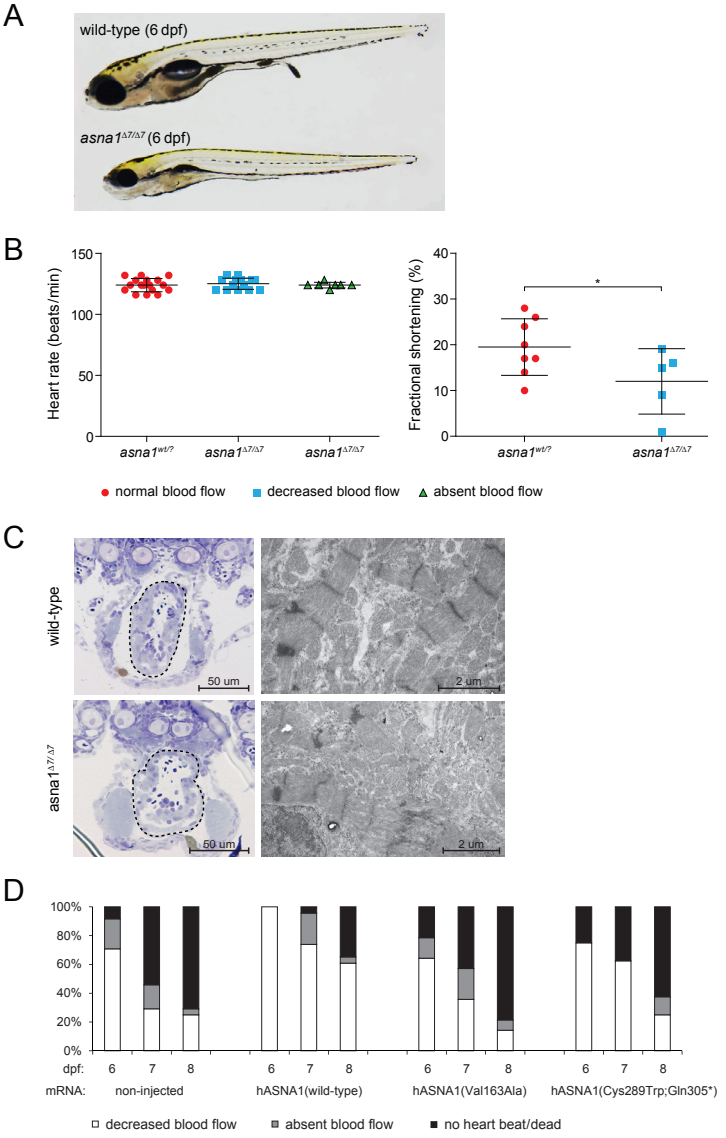

Figure 5. Knockout of *asna1* causes cardiac failure in zebrafish larvae. (A) Lateral view of wild-type and homozygous *asna1* mutant (*asna1*$^{\Delta7/\Delta7}$) larvae at 6 dpf. Overall, *asna1*$^{\Delta7/\Delta7}$ mutants did not show an overt embryonic phenotype besides smaller body size and lack of swim bladder inflation. (B) Quantification of cardiac function in zebrafish larvae. Mean heart rate (beats per minute) did not differ between the groups, even in the absence of blood flow. Fractional shortening was significantly reduced in *asna1*$^{\Delta7/\Delta7}$ mutants compared to wild-type and heterozygous clutchmates (p<0.05). (C) Microscopic imaging of zebrafish hearts. Coronary sections (left) showing abnormal shaped ventricle with thinner wall in *asna1*$^{\Delta7/\Delta7}$ mutant. Electron microscopy images (right) showing myofibrillar disorganization and abnormal intercalated disc ultrastructure in *asna1*$^{\Delta7/\Delta7}$ mutant. (D) From 5 dpf, *asna1*$^{\Delta7/\Delta7}$ mutants showed reduced to absent red blood cell flow rate. At 9 dpf, all *asna1*$^{\Delta7/\Delta7}$ mutants had died. Injection of wild-type human *ASNA1* mRNA significantly ameliorated the phenotype (p<0.005 at all time points), whereas injection of either mutant (Val163Ala or Cys289Trp;Gln305*) mRNA had no significant effect.

Discussion

Our results show that biallelic loss-of-function variants in *ASNA1* cause cardiac septal defects and a rapidly progressive cardiomyopathy resulting in acute heart failure and death in early infancy. We report that *asna1* deficiency in zebrafish also causes cardiac defects and early lethality, which implies that, in vertebrates, the TA protein insertion pathway is specifically critical to development and function of the heart. ASNA1 binds to the transmembrane segment of newly synthesized TA proteins and delivers them to the WRB/CAML receptor complex for insertion into the ER membrane [27]. Together, this complex is essential for efficient and proper targeting of a wide range of TA proteins [28]. Thus far, the corresponding genes *ASNA1* (MIM 601913), *WRB* (MIM 602915) and *CAMLG* (MIM 601118) have not been associated with disease in humans.

Both affected siblings displayed an extraordinary clinical course of DCM, with a sudden, unpredictable onset of heart failure. We postulate that external stressors (e.g. blood withdrawal or infection) or protein aggregation exceeding a critical threshold trigger a cascade of events that result in manifestation of disease. Given the ubiquitous expression of ASNA1 and the fundamental cellular processes TA proteins are involved in, one might expect that biallelic loss-of-function variants in *ASNA1* would have more pleiotropic effects. Indeed, zebrafish mutant for Asna1 or for the Asna1 receptor Wrb have visual function defects and reduced touch response (**Supplemental Table 4**) [29, 30]. In addition, both mouse and zebrafish Wrb mutants have hearing defects due to mislocalization of the TA protein otoferlin, indicating the ASNA1-mediated TA protein insertion is critical in hearing [30, 31]. Moreover, in the nematode *Caenorhabditis elegans*, reduced *asna1* activity causes exocytosis defects leading to defective insulin secretion, which was confirmed in pancreatic mouse *Asna1* knockouts [15, 16]. While no extra-cardiac abnormalities were found in the siblings it is possible that other abnormalities have gone unnoticed, did not yet develop at this early age, or are masked by the low but detectable functionality of the Val163Ala mutant protein.

The prevalence of *ASNA1*-related cardiomyopathy is probably low, given the negative results upon cohort screening (n=70) and the low rate of protein-altering variants in population datasets. Considering the rapidly fatal disease course, additional patients may be found in cases of sudden unexpected infant death, or, assuming that severe impairment of ASNA1 is incompatible with life [11], families with recurrent miscarriage or fetal death.

The nucleotide and amino acid sequences of ASNA1 are highly conserved across vertebrate species (**Figure 1C**). The mouse *Asna1* gene and corresponding protein share 90% nucleotide identity and 100% amino acid identity with its human counterparts. Homozygous *Asna1* knockout mice, though apparently normal at the blastocyst (E3.5) stage, displayed early em-

bryonic lethality [11]. Heterozygous *Asna1* knockout mice, on the other hand, were viable and showed no apparent abnormalities. These findings underscore that *Asna1* plays a crucial role in embryonic development, and that one functional copy of the gene is sufficient for normal development.

We explored the role of *asna1* in cardiac development in the zebrafish. Unlike mice, zebrafish embryos are not dependent upon a functional cardiovascular system for sufficient supply of oxygen but rely on passive diffusion [32]. Embryos with severe cardiovascular defects can therefore be studied past the initial stages of embryonic development. Here, we used CRISPR/Cas9-mediated genome editing to generate a loss-of-function model for *ASNA1* in zebrafish. This strategy resulted in an early cardiac phenotype. CRISPR-mediated *asna1*$^{\Delta 7/\Delta 7}$ knockouts displayed decreased blood flow in the dorsal aorta, impaired cardiac contractility, and premature lethality, recapitulating the heart failure phenotype observed in our patients.

Previous studies in vertebrate models of the WRB-CAMLG receptor complex also point toward a role in cardiac development and disease (**Supplemental Table 4**). Morpholino knockdown of *wrb* in clawed frogs (*Xenopus tropicalis*) and medaka fish (*Oryzias latipalis*) induced cardiac looping defects and abnormal chamber differentiation [12, 14]. Of note, microscopic analysis in *wrb*-deficient frogs revealed large intercellular gaps between cardiomyocytes, reminiscent of the intercalated disc abnormalities observed in our family. These findings suggests that genes encoding other components of the TA protein insertion pathway may be good candidate genes for cardiovascular disease as well.

The exact mechanism by which *ASNA1* variants result in cardiomyopathy remains to be determined. Several TA proteins have been linked to cardiomyopathy (including dysferlin, emerin, junctophilin-2, phospholamban, nesprin-1 and nesprin-2), and failure to correctly localize one or more of these proteins, due to defective ASNA1-mediated membrane insertion, may be responsible for the cardiac phenotype observed in both patients and zebrafish. Intriguingly, variants in the emerin gene (*EMD*), which cause a progressive skeletal muscle weakness and cardiomyopathy known as X-linked Emery-Dreifuss muscular dystrophy (MIM 310300), result in mislocalization of the protein due to impaired ASNA1-mediated nuclear targeting [33]. Though emerin staining showed apparently normal localization of the protein in our patients, it did reveal the characteristic abnormal nuclear morphology previously described in Emery-Dreifuss muscular dystrophy [34] Taken together, we hypothesize that defective ASNA1-mediated targeting affects several cardiomyopathy-related TA proteins, which together may explain the early onset and severity of disease in our patients.

A distinct subset of TA proteins are involved in vesicular trafficking between the ER and Golgi and the secretory machinery, including several SNAP-receptors (SNAREs) and vesicle-

associated membrane proteins (VAMPs) essential for intracellular membrane fusion (**Supplemental Table 3**). Glycosylation of proteins and lipids, a complex process which starts in the ER and continues in the Golgi, highly depends on intracellular vesicular trafficking. Therefore, we postulate that the abnormal isoelectric focusing profiles of transferrin and apoliprotein C III in both our patients results from defective membrane targeting of TA proteins involved in vesicular trafficking and exocytosis.

TA proteins do not solely rely on ASNA1 for insertion into the ER membrane. A subset of TA proteins with moderately hydrophobic transmembrane domains can integrate in the ER membrane via an alternative route dependent on the highly conserved ER membrane protein complex (EMC) [35]. Although other routes have been demonstrated *in vitro* [36, 37], their functional contribution to TA protein insertion in mammalian cells remains unclear at present. These alternative routes might not be effective or sufficient for all TA proteins, in particular strongly hydrophobic TA proteins (such as the vesicle-associated membrane protein 2), or in all cell types, suggesting why certain proteins or tissues might be more severely affected by defective ASNA1-mediated targeting.

Taken together, our study shows that biallelic variants in *ASNA1*, encoding a cytosolic targeting factor for TA proteins, cause severe pediatric DCM with early onset and rapid progression. We hypothesize that this phenotype is caused by mislocalized TA proteins, either by toxic aggregation or reduced levels of functional protein. Our findings point toward a critical role of the TA protein insertion pathway in vertebrate heart function and disease.

Acknowledgements

The authors wish to thank the family members for their participation in this study. We thank Tom de Vries Lentsch (Department of Clinical Genetics, Erasmus MC, University Medical Center Rotterdam) for the photographic artwork, Mike Broeders (Department of Clinical Genetics, Erasmus MC, University Medical Center Rotterdam) for Cas9 protein synthesis, and John O'Donnell (MRC Laboratory of Molecular Biology) for help with thermal stability assays.

References

1. Pinto YM, Elliott PM, Arbustini E, Adler Y, Anastasakis A, Bohm M, et al. Proposal for a revised definition of dilated cardiomyopathy, hypokinetic non-dilated cardiomyopathy, and its implications for clinical practice: a position statement of the ESC working group on myocardial and pericardial diseases. *Eur Heart J.* 2016; 37:1850-1858.
2. Morales A, Hershberger RE. Genetic evaluation of dilated cardiomyopathy. *Curr Cardiol Rep.* 2013;15:375.
3. Lee TM, Hsu DT, Kantor P, Towbin JA, Ware SM, Colan SD, et al. Pediatric Cardiomyopathies. *Circ Res.* 2017; 121:855-873.
4. Rampersaud E, Siegfried JD, Norton N, Li D, Martin E, Hershberger RE. Rare variant mutations identified in pediatric patients with dilated cardiomyopathy. *Prog Pediatr Cardiol.* 2011;31:39-47.
5. Vasilescu C, Ojala TH, Brilhante V, Ojanen S, Hinterding HM, Palin E, et al. Genetic Basis of Severe Childhood-Onset Cardiomyopathies. *J Am Coll Cardiol.* 2018;72:2324-2338.
6. Long PA, Evans JM, Olson TM. Diagnostic Yield of Whole Exome Sequencing in Pediatric Dilated Cardiomyopathy. *J Cardiovasc Dev Dis.* 2017;4:11.
7. Herkert JC, Abbott KM, Birnie E, Meems-Veldhuis MT, Boven LG, Benjamins M, et al. Toward an effective exome-based genetic testing strategy in pediatric dilated cardiomyopathy. *Genet Med.* 2018;
8. Stefanovic S, Hegde RS. Identification of a targeting factor for posttranslational membrane protein insertion into the ER. *Cell.* 2007;128:1147-1159.
9. Hegde RS, Keenan RJ. Tail-anchored membrane protein insertion into the endoplasmic reticulum. *Nat Rev Mol Cell Biol.* 2011;12:787-798.
10. Borgese N, Fasana E. Targeting pathways of C-tail-anchored proteins. *Biochim Biophys Acta.* 2011;1808: 937-946.
11. Mukhopadhyay R, Ho YS, Swiatek PJ, Rosen BP, Bhattacharjee H. Targeted disruption of the mouse Asna1 gene results in embryonic lethality. *FEBS Lett.* 2006;580:3889-3894.
12. Murata K, Degmetich S, Kinoshita M, Shimada E. Expression of the congenital heart disease 5/tryptophan rich basic protein homologue gene during heart development in medaka fish, Oryzias latipes. *Dev Growth Differ.* 2009;51:95-107.
13. Tran DD, Russell HR, Sutor SL, van Deursen J, Bram RJ. CAML is required for efficient EGF receptor recycling. *Dev Cell.* 2003;5:245-256.
14. Sojka S, Amin NM, Gibbs D, Christine KS, Charpentier MS, Conlon FL. Congenital heart disease protein 5 associates with CASZ1 to maintain myocardial tissue integrity. *Development.* 2014;141:3040-3049.
15. Norlin S, Parekh V, Edlund H. The ATPase activity of Asna1/TRC40 is required for pancreatic progenitor cell survival. *Development.* 2018;145
16. Kao G, Nordenson C, Still M, Ronnlund A, Tuck S, Naredi P. ASNA-1 positively regulates insulin secretion in C. elegans and mammalian cells. *Cell.* 2007;128:577-587.
17. Ponikowski P, Voors AA, Anker SD, Bueno H, Cleland JG, Coats AJ, et al. 2016 ESC Guidelines for the diagnosis and treatment of acute and chronic heart failure: The Task Force for the diagnosis and treatment of acute and chronic heart failure of the European Society of Cardiology (ESC)Developed with the special contribution of the Heart Failure Association (HFA) of the ESC. *Eur Heart J.* 2016;37:2129-2200.
18. Li H, Durbin R. Fast and accurate long-read alignment with Burrows-Wheeler transform. *Bioinformatics.* 2010;26:589-595.
19. McKenna A, Hanna M, Banks E, Sivachenko A, Cibulskis K, Kernytsky A, et al. The Genome Analysis Toolkit: a MapReduce framework for analyzing next-generation DNA sequencing data. *Genome Res.* 2010;20: 1297-1303.
20. van Veen TA, van Rijen HV, Wiegerinck RF, Opthof T, Colbert MC, Clement S, et al. Remodeling of gap junctions in mouse hearts hypertrophied by forced retinoic acid signaling. *J Mol Cell Cardiol.* 2002;34: 1411-1423.
21. Shao S, Rodrigo-Brenni MC, Kivlen MH, Hegde RS. Mechanistic basis for a molecular triage reaction. *Science.* 2017;355:298-302.

22. Mateja A, Szlachcic A, Downing ME, Dobosz M, Mariappan M, Hegde RS, et al. The structural basis of tail-anchored membrane protein recognition by Get3. *Nature.* 2009;461:361-366.
23. Kuil LE, Oosterhof N, Geurts SN, van der Linde HC, Meijering E, van Ham TJ. Reverse genetic screen reveals that Il34 facilitates yolk sac macrophage distribution and seeding of the brain. *bioRxiv.* 2018:406553.
24. Hoage T, Ding Y, Xu X. Quantifying cardiac functions in embryonic and adult zebrafish. *Methods Mol Biol.* 2012;843:11-20.
25. The UniProt Consortium. UniProt: the universal protein knowledgebase. *Nucleic Acids Res.* 2017;45:D158-D169.
26. Sikkema-Raddatz B, Johansson LF, de Boer EN, Almomani R, Boven LG, van den Berg MP, et al. Targeted next-generation sequencing can replace Sanger sequencing in clinical diagnostics. *Hum Mutat.* 2013;34:1035-1042.
27. Vilardi F, Stephan M, Clancy A, Janshoff A, Schwappach B. WRB and CAML are necessary and sufficient to mediate tail-anchored protein targeting to the ER membrane. *PLoS One.* 2014;9:e85033.
28. Schuldiner M, Metz J, Schmid V, Denic V, Rakwalska M, Schmitt HD, et al. The GET complex mediates insertion of tail-anchored proteins into the ER membrane. *Cell.* 2008;134:634-645.
29. Daniele LL, Emran F, Lobo GP, Gaivin RJ, Perkins BD. Mutation of wrb, a Component of the Guided Entry of Tail-Anchored Protein Pathway, Disrupts Photoreceptor Synapse Structure and Function. *Invest Ophthalmol Vis Sci.* 2016;57:2942-2954.
30. Lin SY, Vollrath MA, Mangosing S, Shen J, Cardenas E, Corey DP. The zebrafish pinball wizard gene encodes WRB, a tail-anchored-protein receptor essential for inner-ear hair cells and retinal photoreceptors. *J Physiol.* 2016;594:895-914.
31. Vogl C, Panou I, Yamanbaeva G, Wichmann C, Mangosing SJ, Vilardi F, et al. Tryptophan-rich basic protein (WRB) mediates insertion of the tail-anchored protein otoferlin and is required for hair cell exocytosis and hearing. *Embo J.* 2016;35:2536-2552.
32. Brown DR, Samsa LA, Qian L, Liu J. Advances in the Study of Heart Development and Disease Using Zebrafish. *J Cardiovasc Dev Dis.* 2016;3
33. Pfaff J, Rivera Monroy J, Jamieson C, Rajanala K, Vilardi F, Schwappach B, et al. Emery-Dreifuss muscular dystrophy mutations impair TRC40-mediated targeting of emerin to the inner nuclear membrane. *J Cell Sci.* 2016;129:502-516.
34. Fidzianska A, Hausmanowa-Petrusewicz I. Architectural abnormalities in muscle nuclei. Ultrastructural differences between X-linked and autosomal dominant forms of EDMD. *J Neurol Sci.* 2003;210:47-51.
35. Guna A, Volkmar N, Christianson JC, Hegde RS. The ER membrane protein complex is a transmembrane domain insertase. *Science.* 2018;359:470-473.
36. Brambillasca S, Yabal M, Makarow M, Borgese N. Unassisted translocation of large polypeptide domains across phospholipid bilayers. *J Cell Biol.* 2006;175:767-777.
37. Casson J, McKenna M, Hassdenteufel S, Aviram N, Zimmerman R, High S. Multiple pathways facilitate the biogenesis of mammalian tail-anchored proteins. *J Cell Sci.* 2017;130:3851-3861.

Supplemental Information

Detailed Methods

Purification of recombinant ASNA1

The Rosetta BL21(DE3) pLysS strain of *E. coli* (Novagen) was transformed with the plasmid for wild-type or mutant ASNA1, and a single colony was used to grow an overnight starter culture. This was expanded to either 1 L or 6 L (for the wild-type and mutant cultures, respectively), and when the absorbance at 600 nm was between 0.4 to 0.6, isopropyl β-D-1-thiogalactopyranoside (IPTG) was added to 1 mM. After 3 hours at 37°C, the cells were collected by centrifugation at 4°C, washed once in ice cold PBS supplemented with 250 mM NaCl, and re-collected by centrifugation. The washed cells were resuspended in 35 mL of ice cold lysis buffer [PBS with 250 mM NaCl, 5 mM 2-mercaptoethanol, and 1X cOmplete EDTA-free Protease Inhibitor Cocktail mix (Roche)]. After lysis by sonication, the insoluble material was sedimented by centrifugation at 18,000 rpm for 30 minutes at 4°C. The soluble extract was adjusted to 20 mM imidazole, then passed over a 3 mL column of Ni-NTA resin, washed three times in 10 mL of lysis buffer supplemented with 20 mM imidazole, and eluted with lysis buffer supplemented with 250 mM imidazole. The peak fractions (identified by absorbance at 280 nm) were pooled, mixed with TEV protease (at a protein ratio of 1:100), and dialyzed overnight against dialysis buffer (150 mM KAc, 50 mM HEPES, pH 7.4, 2 mM MgCl2, 10% glycerol, 7 mM 2-mercaptoethanol). Insoluble material was removed by centrifugation, and the dialyzed sample was passed over a 3 mL column of Ni-NTA to remove the cleaved tag and TEV protease. The flow-through was collected and concentrated to ~4 mg/mL by centrifugal concentrators (Amicon). The protein was snap-frozen in liquid nitrogen and stored in aliquots at -80°C.

Analysis of ASNA1 protein function in vitro

^{35}S-labeled TA protein containing the transmembrane domain of VAMP2 (referred to simply as VAMP2 hereinafter) was assembled with the upstream chaperone SGTA. The TA protein contained a photo-crosslinking residue within the transmembrane domain to monitor its interactions. The SGTA-VAMP2 complex was then mixed with the bridging cBAG6 complex and either wild-type or mutant ASNA1. After incubating at 32°C for 90 seconds, the reaction was transferred to ice and irradiated with UV to induce crosslinking for 10 minutes. The samples were analyzed by SDS-PAGE and autoradiography to determine whether VAMP2 was successfully transferred from SGTA to ASNA1. To test the functionality of ASNA1 for TA protein insertion, a complex between ASNA1 and VAMP2 was assembled as before [1], and incubated with ER microsomes for between 0 to 15 minutes at 32°C. The samples were then analyzed by SDS-PAGE and autoradiography. Insertion of the TA protein was monitored by its glycosylation at a site located near the C-terminus. The ER microsomes used for this assay were derived from HEK293 cells and were prepared as described before [2].

Zebrafish care and maintenance

Zebrafish (*Danio rerio*) were raised and maintained under standard conditions at 28°C [3]. All zebrafish experiments were performed in compliance with Dutch animal welfare legislation. Study protocols were approved by the institutional review board for experimental animals.

CRISPR/Cas9 targeting of zebrafish asna1

The online program CRISPRscan (www.crisprscan.org) was used to used to design a single-stranded guide RNA (gRNA) targeting exon 5 in *asna1* (5'-CCAAACTGGAGGAGACGCTGC-3'), approximately in between the variants identified in the parents. The gRNAs were obtained by *in vitro* transcription of synthetic oligonucleotides containing a minimal T7 RNA polymerase promoter using the mMESSAGE mMACHINE T7 Ultra Kit (Thermo Fisher Scientific). SP-Cas9 plasmid was a gift from Niels Geijssen (Addgene plasmid #62731) [4]. A mix of 100 pg of either gRNA and 650 pg Cas9 protein was injected into single-cell stage zebrafish embryos. Injected embryos were raised to adulthood (F0) and analyzed for genomic modifications at the target site by Sanger sequencing and the online tool Tracking Indel by DEcompensition (TIDE) [5]. In two individual F0 founder fish, ~30% of the mapped reads contained indels at the target site in exon 5 (**Supplemental Figure 1**). We screened their offspring (F1) for germline transmission using PCR followed by restriction enzyme digestion (**Supplemental Table 2**), and identified three fish (25%) that carried a heterozygous 7 base pair deletion (Δ7). These fish were used for further breeding to create a stable mutant line. For rescue experiments, 300 pg wild-type or mutant human *ASNA1* mRNA (see above) was injected in the yolk at the single-cell stage. Expression of MYC-tagged human ASNA1 was confirmed by Western blot analysis with an anti-MYC primary antibody.

Supplemental Table 1. List of primer sequences used for Sanger sequencing

Target	Direction	Primer sequence (5′ - 3′)	Amplicon size
ASNA1 exon 1	F	tcctaaaaggcaagtaatgagga	367
	R	gtggaaaagccggtccttg	
ASNA1 exon 2	F	ctgctccagggaacctacc	389
	R	tggttcccttgtgagtatgttg	
ASNA1 exon 3	F	ccccttgtttttgacccttt	470
	R	AAGTTCATGCCCTTCACCAG	
ASNA1 exon 4	F	ATCGATGAGGCCATGAGCTA	375
	R	tgggaaggaaagggaattgt	
ASNA1 exon 5	F	ccactgggaggtatcaggag	599
	R	caggaggctagagggcagag	
ASNA1 exon 6	F	TCAAGGACCCTgtgagtgg	400
	R	caggaggctagagggcagag	
ASNA1 exon 7	F	cactctgtctctgccttcctg	299
	R	GGCTCCCCCTGTATTATGG	

F, forward; R, reverse.

Supplemental Table 2. List of oligonucleotide sequences used in zebrafish studies

Target	Direction	Primer sequence (5′ - 3′)	Amplicon size
asna1 exon 5	F	TAAAGCCCATTCCTGAGTGC	404
	R	TTGAAGTGGATGGATGATGG	

F, forward; R, reverse. The PCR product was subjected to restriction enzyme digestion by BsrI. As a result of the 7 bp deletion induced by CRISPR/Cas9, one BsrI enzyme restriction site will be lost and the mutant allele will only be cut once. Subsequent gel electrophoresis will reveal three bands in wild-type (199, 131 and 74 bp), four bands in *asna1*$^{\Delta 7/+}$ (266, 199, 131 and 74 bp), and two bands in *asna1*$^{\Delta 7/\Delta 7}$ (266 and 131 bp) zebrafish.

Supplemental Table 3. List of predicted human tail-anchored proteins

Entry	Protein names	TMD sequence
E0CX11	Short transmembrane mitochondrial protein 1	GFTLGNVVGMYLAQNYD
Q8NDB6	Protein FAM156A/FAM156B (Transmembrane protein 29/29B)	WETLVQGLSGLTLSLGT
Q9H7X2	Uncharacterized protein C1orf115	VVIGLQGFAAAYSAPFAVATSVV
Q8TCY0	Small integral membrane protein 11B	MEFPLCGCLSLILHHFA
Q96PS6	Putative uncharacterized protein GAFA-1 (Gene associated with FGF-2 activity protein 1)	IHLYVMASAMSSSPIFFFFQ
O75438	NADH dehydrogenase [ubiquinone] 1 beta subcomplex subunit 1 (Complex I-MNLL) (CI-MNLL) (NADH-ubiquinone oxidoreductase MNLL subunit)	HWVHVLVPMGFVIGCYL
Q9H1C7	Cysteine-rich and transmembrane domain-containing protein 1	LGPSTCLTACWTALCCCC
Q9HDD0	Phospholipid-metabolizing enzyme A-C1 (EC 2.3.1.-) (EC 3.1.1.-) (HRAS-like suppressor 1) (HRSL1)	ISTVEFVTAAVGVFSFLGLFPKGQ
L0R6Q1	SLC35A4 upstream open reading frame protein	ASAVLGFAVGTCTGIYAAQAYAV
Q96I36	Cytochrome c oxidase assembly protein COX14	FSTSMMLLTVYGGYLCSVRVYHY
P21397	Amine oxidase [flavin-containing] A (EC 1.4.3.4) (Monoamine oxidase type A) (MAO-A)	VSGLLKIIGFSTSVTALGFVL
O75452	Retinol dehydrogenase 16 (EC 1.1.-.-) (Microsomal NAD(+)-dependent retinol dehydrogenase 4) (RoDH-4) (Short chain dehydrogenase/ reductase family 9C member 8) (Sterol/retinol dehydrogenase)	LLYLPMSYMPTFLVDAIMYWV
Q9BVW6	Small integral membrane protein 2	GHAISILFGFWTSFICDTYIVLA
Q75NE6	Putative microRNA 17 host gene protein (Putative microRNA host gene 1 protein)	LNVPKLVLIYLQSHFVLFFFSMC
Q9UMX3	Bcl-2-related ovarian killer protein (hBOK) (Bcl-2-like protein 9) (Bcl2-L-9)	WLVAALCSFGRFLKAAFFVLL
Q8TCP9	Protein FAM200A	ILLLLPFTTTYLCELGFSIL
O95167	NADH dehydrogenase [ubiquinone] 1 alpha subcomplex subunit 3 (Complex I-B9) (CI-B9) (NADH-ubiquinone oxidoreductase B9 subunit)	LVVSFVVGGLAVILPPLSPYF
Q07812	Apoptosis regulator BAX (Bcl-2-like protein 4) (Bcl2-L-4)	TVTIFVAGVLTASLTIWKKMG
Q8WXE9	Stonin-2 (Stoned B)	IWLMLPTPFVHPTTLPLLFLLAM
Q9NX95	Syntabulin (Golgi-localized syntaphilin-related protein) (Syntaxin-1-binding protein)	SFLVDLLAVAAPVVPTVLWAF
Q6ZSY5	Protein phosphatase 1 regulatory subunit 3F (R3F)	VLAGLVVVPVALNSGVSLLVL
Q3KP22	Membrane-anchored junction protein	AATGFFGFLSSLFPFRYFF
A8MTT3	Protein CEBPZOS (CEBPZ antisense RNA 1) (CEBPZ opposite strand)	GVLVAELVGVFGAYFLFS
Q07817	Bcl-2-like protein 1 (Bcl2-L-1) (Apoptosis regulator Bcl-X)	FNRWFLTGMTVAGVVLL
P56378	6.8 kDa mitochondrial proteolipid	VYQEIWIGMGLMGFIVYKI
O15079	Syntaphilin	YIVDLLAVVVPAVPTVAWLC
Q9NRY6	Phospholipid scramblase 3 (PL scramblase 3) (Ca(2+)-dependent phospholipid scramblase 3)	VKAVLLGATFLIDYMFF
Q9NUB4	Uncharacterized protein C20orf141	LLLLMGLGPLLRACGMPLTLL
O95139	NADH dehydrogenase [ubiquinone] 1 beta subcomplex subunit 6 (Complex I-B17) (CI-B17) (NADH-ubiquinone oxidoreductase B17 subunit)	SIFVFTHVLVPVWIIHYYM
O43676	NADH dehydrogenase [ubiquinone] 1 beta subcomplex subunit 3 (Complex I-B12) (CI-B12) (NADH-ubiquinone oxidoreductase B12 subunit)	VFFKGFKWGFAAFVVAVGAEYYL

Supplemental Table 3. List of predicted human tail-anchored proteins (*continued*)

Entry	Protein names	TMD sequence
Q8NCU8	Uncharacterized protein encoded by LINC00116	LQLSVLVAFASGVLLGW
Q8N4H5	Mitochondrial import receptor subunit TOM5 homolog	SIRNFLIYVALLRVTPFIL
Q9NRY7	Phospholipid scramblase 2 (PL scramblase 2) (Ca(2+)-dependent phospholipid scramblase 2)	MKAVMIGACFLIDYMFF
Q8N7S6	Uncharacterized protein ARIH2OS (Ariadne-2 homolog opposite strand protein)	CILTALLAVSFHSIGVVIMTS
Q9UL19	Retinoic acid receptor responder protein 3 (EC 3.1.1.-) (HRAS-like suppressor 4) (HRSL4) (RAR-responsive protein TIG3) (Retinoid-inducible gene 1 protein) (Tazarotene-induced gene 3 protein)	KVEVGVATALGILVVAGCSFAI
A2RU48	Single-pass membrane and coiled-coil domain-containing protein 3	IGASLLGSIGVAVLGLGIDMI
P03928	ATP synthase protein 8 (A6L) (F-ATPase subunit 8)	VWPTMITPMLLTLFLIT
P0DJ07	Protein PET100 homolog, mitochondrial	IFRMIIYLTFPVAMFWVS
Q5TGZ0	MICOS complex subunit MIC10 (Mitochondrial inner membrane organizing system protein 1)	AVVKIGTGFGLGIVFSLTFF
O15162	Phospholipid scramblase 1 (PL scramblase 1) (Ca(2+)-dependent phospholipid scramblase 1) (Erythrocyte phospholipid scramblase) (MmTRA1b)	MKAVMIGACFLIDFMFF
O15239	NADH dehydrogenase [ubiquinone] 1 alpha subcomplex subunit 1 (Complex I-MWFE) (CI-MWFE) (NADH-ubiquinone oxidoreductase MWFE subunit)	MWFEILPGLSVMGVCLLIPGL
A6NCI5	Putative transmembrane protein encoded by LINC00862 (Small integral membrane protein 16)	IMALILMPSLHCFGNILILLF
Q9NRQ2	Phospholipid scramblase 4 (PL scramblase 4) (Ca(2+)-dependent phospholipid scramblase 4) (Cell growth-inhibiting gene 43 protein) (TRA1)	MKAMIFGACFLIDFMYF
Q9BSJ5	Uncharacterized protein C17orf80 (Cell migration-inducing gene 3 protein) (Human lung cancer oncogene 8 protein) (HLC-8)	GFGGITMLFTGYFVLCCSWSF
P08574	Cytochrome c1, heme protein, mitochondrial (Complex III subunit 4) (Complex III subunit IV) (Cytochrome b-c1 complex subunit 4) (Ubiquinol-cytochrome-c reductase complex cytochrome c1 subunit) (Cytochrome c-1)	MLMMMALLVPLVYTI
Q9HD87	Putative uncharacterized protein C6orf50 (Nasopharyngeal carcinoma-associated gene 19 protein)	IISLLAIFIKMCLWLWKQFL
P60602	Reactive oxygen species modulator 1 (ROS modulator 1) (Epididymis tissue protein Li 175) (Glyrichin) (Mitochondrial targeting GxxxG motif protein) (MTGM) (Protein MGR2 homolog)	GFVMGCAVGMAAGALFGTFSCLR
Q9P0U1	Mitochondrial import receptor subunit TOM7 homolog (Translocase of outer membrane 7 kDa subunit homolog)	FAIRWGFIPLVIYLGF
P0DMW3	Small integral membrane protein 10-like protein 1	FFYFYILASVILNVHLQVY
Q96HG1	Small integral membrane protein 10	FFYFYILASVILNVHLQVY
Q96IX5	Up-regulated during skeletal muscle growth protein 5 (Diabetes-associated protein in insulin-sensitive tissues) (HCV F-transactivated protein 2)	TLTGRMNCVLATYGSIALIVLYF
O95237	Lecithin retinol acyltransferase (EC 2.3.1.135) (Phosphatidylcholine--retinol O-acyltransferase)	VLASAVLGLASIVCTGLVSYT
E9PQ53	NADH dehydrogenase [ubiquinone] 1 subunit C2, isoform 2 (NDUFC2-KCTD14 readthrough transcript protein)	GLHRQLLYITAFFFAGYYLV
O95298	NADH dehydrogenase [ubiquinone] 1 subunit C2 (Complex I-B14.5b) (CI-B14.5b) (Human lung cancer oncogene 1 protein) (HLC-1) (NADH-ubiquinone oxidoreductase subunit B14.5b)	GLHRQLLYITAFFFAGYYLV
P56134	ATP synthase subunit f, mitochondrial	ISGITMVLACYVLFSYSFSY
A0A5B9	T-cell receptor beta-2 chain C region	TILYEILLGKATLYAVLVSALVL

Supplemental Table 3. List of predicted human tail-anchored proteins (*continued*)

Entry	Protein names	TMD sequence
P53816	HRAS-like suppressor 3 (HRSL3) (EC 3.1.1.32) (EC 3.1.1.4) (Adipose-specific phospholipase A2) (AdPLA) (Group XVI phospholipase A1/A2) (H-rev 107 protein homolog) (H-REV107) (HREV107-1) (HRAS-like suppressor 1) (HREV107-3) (Renal carcinoma antigen NY-REN-65)	VIIAASVAGMGLAAMSLIGVMFS
Q7Z412	Peroxisome assembly protein 26 (Peroxin-26)	FFSLPFKKSLLAALILCLLVV
Q9NS69	Mitochondrial import receptor subunit TOM22 homolog (hTom22) (1C9-2) (Translocase of outer membrane 22 kDa subunit homolog)	ALWIGTTSFMILVLPVVFET
Q9GZY8	Mitochondrial fission factor	VMYSITVAFWLLNSWLWF
Q13505	Metaxin-1 (Mitochondrial outer membrane import complex protein 1)	ILSVLAGLAAMVGYALLSGIV
P01848	T-cell receptor alpha chain C region	VIGFRILLLKVAGFNLLMTL
P27338	Amine oxidase [flavin-containing] B (EC 1.4.3.4) (Monoamine oxidase type B) (MAO-B)	PGLLRLIGLTTIFSATALGFLAHKRGL
O00198	Activator of apoptosis harakiri (BH3-interacting domain-containing protein 3) (Neuronal death protein DP5)	WPWLCAAAQVAALAAWLLG
B7Z8K6	T-cell receptor delta chain C region	LGLRMLFAKTVAVNFLLTAKLFF
O95168	NADH dehydrogenase [ubiquinone] 1 beta subcomplex subunit 4 (Complex I-B15) (CI-B15) (NADH-ubiquinone oxidoreductase B15 subunit)	LMGALCGFGPLIFIYYII
Q16611	Bcl-2 homologous antagonist/killer (Apoptosis regulator BAK) (Bcl-2-like protein 7) (Bcl2-L-7)	ILNVLVVLGVVLLGQFVV
O60238	BCL2/adenovirus E1B 19 kDa protein-interacting protein 3-like (Adenovirus E1B19K-binding protein B5) (BCL2/adenovirus E1B 19 kDa protein-interacting protein 3A) (NIP3-like protein X) (NIP3L)	VFIPSLFLSHVLALGLGIYIG
Q96N68	Putative uncharacterized protein C18orf15	MCVCVHVCACVYVCMCVLVCM
Q07820	Induced myeloid leukemia cell differentiation protein Mcl-1 (Bcl-2-like protein 3) (Bcl2-L-3) (Bcl-2-related protein EAT/mcl1) (mcl1/EAT)	IRNVLLAFAGVAGVGAGLAYL
Q09013	Myotonin-protein kinase (MT-PK) (EC 2.7.11.1) (DM-kinase) (DMK) (DM1 protein kinase) (DMPK) (Myotonic dystrophy protein kinase)	LLLFAVVLSRAAALGCIGLVA
Q9Y3D6	Mitochondrial fission 1 protein (FIS1 homolog) (hFis1) (Tetratricopeptide repeat protein 11) (TPR repeat protein 11)	LVGMAIVGGMALGVAGLAGLI
Q96JJ6	Junctophilin-4 (JP-4) (Junctophilin-like 1 protein)	LVVGAVALLDLSLAFLFSQLLT
Q96K12	Fatty acyl-CoA reductase 2 (EC 1.2.1.84) (Male sterility domain-containing protein 1)	NIHYLFNTALFLIAWRLLIA
Q9H0X9	Oxysterol-binding protein-related protein 5 (ORP-5) (OSBP-related protein 5) (Oxysterol-binding protein homolog 1)	SWFLLCVFLACQLFINHIL
F7VJQ1	Alternative prion protein (AltPrP)	WWWLGAASWWWLGAAPWWWLG
Q96KF7	Small integral membrane protein 8	PVMAFGLVTLSLCVAYIGYLHAI
Q8WVI0	Small integral membrane protein 4	FGIYRFLPFFFVLGGTMEWIMI
P37268	Squalene synthase (SQS) (SS) (EC 2.5.1.21) (FPP:FPP farnesyltransferase) (Farnesyl-diphosphate farnesyltransferase)	PIYLSFVMLLAALSWQYLTTL
Q3B7S5	Small integral membrane protein 21	HIRFFTLLVLFHVMVLL
P10415	Apoptosis regulator Bcl-2	FSWLSLKTLLSLALVGACITLG
H7C350	Coiled-coil domain-containing protein 188	LLLGALLVWTAAYVYVV
Q14318	Peptidyl-prolyl cis-trans isomerase FKBP8 (PPIase FKBP8) (EC 5.2.1.8) (38 kDa FK506-binding protein) (38 kDa FKBP) (FKBP-38) (hFKBP38) (FK506-binding protein 8) (FKBP-8) (FKBPR38) (Rotamase)	WLFGATAVALGGVALSVVIAA
Q8IVJ8	AP20 region protein 1	IALALAGPGAILILELSWFLG
P0DMT0	Myoregulin	VGRLLKILFVIFVDLISIIYV

Supplemental Table 3. List of predicted human tail-anchored proteins (*continued*)

Entry	Protein names	TMD sequence
Q8N326	Uncharacterized protein C10orf111	MSLLLLPAFSGLTWAPFLFLF
P60059	Protein transport protein Sec61 subunit gamma	FQKIAMATAIGFAIMGFIGFFVKLIHIPI
Q12983	BCL2/adenovirus E1B 19 kDa protein-interacting protein 3	VFLPSLLLSHLLAIGLGIYIG
O43677	NADH dehydrogenase [ubiquinone] 1 subunit C1, mitochondrial (Complex I-KFYI) (CI-KFYI) (NADH-ubiquinone oxidoreductase KFYI subunit)	WLKVGFTLGTTVFLWIYLI
Q8N2K1	Ubiquitin-conjugating enzyme E2 J2 (EC 2.3.2.23) (E2 ubiquitin-conjugating enzyme J2) (Non-canonical ubiquitin-conjugating enzyme 2) (NCUBE-2)	GLLGGALANLFVIVGFAAFAY
O96011	Peroxisomal membrane protein 11B (Peroxin-11B) (Peroxisomal biogenesis factor 11B) (Protein PEX11 homolog beta) (PEX11-beta)	GIVGLCGLVSSILSILTLIYPWL
Q86T96	E3 ubiquitin-protein ligase RNF180 (EC 2.3.2.27) (RING finger protein 180) (RING-type E3 ubiquitin transferase RNF180)	MVIIYIYSVNWVIGFIVFCFL
Q5T8D3	Acyl-CoA-binding domain-containing protein 5	GVLTFAIIWPFIAQWLVYLYY
Q9H4I9	Essential MCU regulator, mitochondrial (Single-pass membrane protein with aspartate-rich tail 1, mitochondrial)	FGLLRVFSIVIPFLYVGTLI
Q8NA58	Poly(A)-specific ribonuclease PNLDC1 (EC 3.1.13.4) (PARN-like domain-containing protein 1) (Poly(A)-specific ribonuclease domain-containing protein 1) (HsPNLDC1)	VNCLLQVCGIVTAWALLAFIL
O95169	NADH dehydrogenase [ubiquinone] 1 beta subcomplex subunit 8, mitochondrial (Complex I-ASHI) (CI-ASHI) (NADH-ubiquinone oxidoreductase ASHI subunit)	LFGFLAFMIFMCWVGDVYPVY
O94966	Ubiquitin carboxyl-terminal hydrolase 19 (EC 3.4.19.12) (Deubiquitinating enzyme 19) (Ubiquitin thioesterase 19) (Ubiquitin-specific-processing protease 19) (Zinc finger MYND domain-containing protein 9)	FVLGTVAALVALVLNVFYPLV
P01850	T-cell receptor beta-1 chain C region	ILLGKATLYAVLVSALVLMAM
Q96A26	Protein FAM162A (E2-induced gene 5 protein) (Growth and transformation-dependent protein) (HGTD-P)	ISYLMIALTVVGCIFMVI
Q969F0	Fetal and adult testis-expressed transcript protein (Cancer/testis antigen 43) (CT43) (Tumor antigen BJ-HCC-2)	TLIIAVLVSASIANLWLWM
Q8N5G0	Small integral membrane protein 20 (Mitochondrial translation regulation assembly intermediate of cytochrome c oxidase protein of 7 kDa) (MITRAC7)	TALIFGGFISLIGAAFYPIYF
Q86UQ5	Gilles de la Tourette syndrome chromosomal region candidate gene 1 protein	AICMEVFLFLWFIAPIYACVC
P00167	Cytochrome b5 (Microsomal cytochrome b5 type A) (MCB5)	WWTNWVIPAISAVAVALMYRLYM
Q9NPU4	Uncharacterized protein C14orf132	AVLLWIAIIATLGNIVVVGVV
P60468	Protein transport protein Sec61 subunit beta	VPVLVMSLLFIASVFMLHIWG
Q9NWW9	HRAS-like suppressor 2 (EC 2.3.1.-) (EC 3.1.1.-)	AVTTVGVAAGLLAAASLVGILLA
Q7Z3B0	Small integral membrane protein 15	YGFLTTVILALTPLFLASAVL
Q9Y5L2	Hypoxia-inducible lipid droplet-associated protein (Hypoxia-inducible gene 2 protein)	LYLLGVVLTLLSIFVRV
Q96FB5	Protein RRNAD1 (Ribosomal RNA adenine dimethylase domain-containing protein 1)	VVAFFSLALLLAPLVETLILL
B2RUZ4	Small integral membrane protein 1 (Vel blood group antigen)	LGIAMKVLGGVALFWIIFILG
Q9Y2R0	Cytochrome c oxidase assembly factor 3 homolog, mitochondrial (Coiled-coil domain-containing protein 56) (Mitochondrial translation regulation assembly intermediate of cytochrome c oxidase protein of 12 kDa)	IVTGLGIGALVLAIYGYTFYS
Q8IXI1	Mitochondrial Rho GTPase 2 (MIRO-2) (hMiro-2) (EC 3.6.5.-) (Ras homolog gene family member T2)	GLLGVVGAAVAAVLSFSLYRVLV

Supplemental Table 3. List of predicted human tail-anchored proteins (*continued*)

Entry	Protein names	TMD sequence
P0C6T2	Dolichyl-diphosphooligosaccharide--protein glycosyltransferase subunit 4	VQLAIFANMLGVSLFLLVVLY
Q14BN4	Sarcolemmal membrane-associated protein (Sarcolemmal-associated protein)	WMPMLAALVAVTAIVLYVPGL
Q8WVX9	Fatty acyl-CoA reductase 1 (EC 1.2.1.84) (Male sterility domain-containing protein 2)	IRYGFNTILVILIWRIFI
Q14D33	Receptor-transporting protein 5 (3CxxC-type zinc finger protein 5) (CXXC-type zinc finger protein 11)	FWIWVSMTVCVFWLMCM
Q8NI28	Putative uncharacterized protein encoded by LINC01006 (Long intergenic non-protein coding RNA 1006)	WIPLLLVAGCVSCFVGLAVCV
I3L1I5	Putative uncharacterized protein LOC100996504	VLSIILLGSLLMCASSFCFAL
A4D256	Dual specificity protein phosphatase CDC14C (EC 3.1.3.16) (EC 3.1.3.48) (CDC14 cell division cycle 14 homolog C)	ILLPSPLAVLTFTLCSVVIWWIV
Q9Y385	Ubiquitin-conjugating enzyme E2 J1 (EC 2.3.2.23) (E2 ubiquitin-conjugating enzyme J1) (Non-canonical ubiquitin-conjugating enzyme 1) (NCUBE-1) (Yeast ubiquitin-conjugating enzyme UBC6 homolog E) (HsUBC6e)	DHGGSAVLIVILTLALAALIF
Q6ZS62	Colorectal cancer-associated protein 1	LYGCFCVGLVSGMAISVLLLA
A6NFE2	Single-pass membrane and coiled-coil domain-containing protein 2	IFIMFDVLTVTGLLCYILFFG
Q9NS64	Protein reprimo	VVQIAVMCVLSLTVVFGIFFL
Q16821	Protein phosphatase 1 regulatory subunit 3A (Protein phosphatase 1 glycogen-associated regulatory subunit) (Protein phosphatase type-1 glycogen targeting subunit) (RG1)	YFLLFLIFLITVYHYDLMIGL
Q9NQG1	Protein MANBAL	YGLFLGAIFQLICVLAIIVPI
P58511	Small integral membrane protein 11A	PLLLYILAAKTLILCLTFAGVKM
Q9Y228	TRAF3-interacting JNK-activating modulator (TRAF3-interacting protein 3)	WLPVLMVVIAAALAVFLA
Q9BXU9	Calcium-binding protein 8 (CaBP8) (Calneuron I) (Calneuron-1)	LICAFAMAFIISVMLIAANQI
A6NL05	Protein FAM74A7	LSLLLHLAVFLWIIIAINFSN
Q4VXF1	Putative protein FAM74A3	LSLLLHLAVFLWIIIAINFSN
Q5RGS3	Protein FAM74A1	LSLLLHLAVFLWIIIAINFSN
Q5T6X4	Protein FAM162B	VKACYIMIGLTIIACFAVIVS
Q9NXE4	Sphingomyelin phosphodiesterase 4 (EC 3.1.4.12) (Neutral sphingomyelinase 3) (nSMase-3) (nSMase3) (Neutral sphingomyelinase III)	LLLAFFVASLFCVGPLPCTLL
P51648	Fatty aldehyde dehydrogenase (EC 1.2.1.3) (Aldehyde dehydrogenase 10) (Aldehyde dehydrogenase family 3 member A2) (Microsomal aldehyde dehydrogenase)	LGLLLLTFLGIVAAVLV
Q8IXI2	Mitochondrial Rho GTPase 1 (MIRO-1) (hMiro-1) (EC 3.6.5.-) (Rac-GTP-binding protein-like protein) (Ras homolog gene family member T1)	WLRASFGATVFAVLGFAMYKALL
Q8N4K4	Reprimo-like protein	VAQIAVLCVLSLTVVFGVFFL
Q8N6R1	Stress-associated endoplasmic reticulum protein 2 (Ribosome-associated membrane protein RAMP4-2)	GPWLLALFVFVVCGSAIFQII
P58549	FXYD domain-containing ion transport regulator 7	TVQTVGMTLATILFLLGILIVIS
Q86V35	Calcium-binding protein 7 (CaBP7) (Calneuron II) (Calneuron-2)	LICAFAIAFIISVMLIAANQV
Q6ZNB6	NF-X1-type zinc finger protein NFXL1 (Ovarian zinc finger protein) (hOZFP)	YYLISVCGVVVVVFAWYI
O75056	Syndecan-3 (SYND3)	AVIVGGVVGALFAAFLVTLLI

Supplemental Table 3. List of predicted human tail-anchored proteins (*continued*)

Entry	Protein names	TMD sequence
P03986	T-cell receptor gamma-2 chain C region (T-cell receptor gamma chain C region PT-gamma-1/2)	MYLLLLLKSVVYFAIITCCLL
A1L1A6	Immunoglobulin superfamily member 23	LLAAGILGAGALIAGMCFIII
Q8N5Y8	Mono [ADP-ribose] polymerase PARP16 (EC 2.4.2.30) (ADP-ribosyltransferase diphtheria toxin-like 15) (Poly [ADP-ribose] polymerase 16) (PARP-16)	SHWFTVMISLYLLLLLIVSVI
P61266	Syntaxin-1B (Syntaxin-1B1) (Syntaxin-1B2)	IMIIICCVVLGVVLASSIGGTLGL
Q9BZF1	Oxysterol-binding protein-related protein 8 (ORP-8) (OSBP-related protein 8)	YFIIFLLILLQVIINFMF
A6NGB0	Transmembrane protein 191C	VLGALQVLLTLPLLFLGLSLL
P0C7N4	Transmembrane protein 191B	VLGALQVLLTLPLLFLGLSLL
Q7Z419	E3 ubiquitin-protein ligase RNF144B (EC 2.3.2.-) (IBR domain-containing protein 2) (RING finger protein 144B) (p53-inducible RING finger protein)	VVGILVGLGIIALVTSPLLLL
Q9UPX6	UPF0258 protein KIAA1024	IAALIAAAACTVILVIVVPIC
P54710	Sodium/potassium-transporting ATPase subunit gamma (Na(+)/K(+) ATPase subunit gamma) (FXYD domain-containing ion transport regulator 2) (Sodium pump gamma chain)	GGLIFAGLAFIVGLLILL
Q96LL3	Uncharacterized protein C16orf92	PGLFHHILVGLLVVAFFFLLF
Q9Y6X1	Stress-associated endoplasmic reticulum protein 1 (Ribosome-attached membrane protein 4)	GPWLLALFIFVVCGSAIFQII
Q16623	Syntaxin-1A (Neuron-specific antigen HPC-1)	IMIIICCVILGIVIASTVGGI
P60509	Endogenous retrovirus group PABLB member 1 Env polyprotein (Endogenous retrovirus group PABLB member 1) (Envelope polyprotein) (HERV-R(b) Env protein) (HERV-R(b)_3p24.3 provirus ancestral Env polyprotein) [Includes: Surface protein domain (SU); Transmembrane protein domain (TM)]	ILIVLATLWSVGIALCCGLYF
P50876	E3 ubiquitin-protein ligase RNF144A (EC 2.3.2.-) (RING finger protein 144A) (UbcM4-interacting protein 4) (Ubiquitin-conjugating enzyme 7-interacting protein 4)	VVGIFAGFGLLLLVASPFLLL
Q96DX8	Receptor-transporting protein 4 (28 kDa interferon-responsive protein) (3CxxC-type zinc finger protein 4)	PLNICVFILLLVFIVVKCFTS
Q12846	Syntaxin-4 (Renal carcinoma antigen NY-REN-31)	IAICVSITVVLLAVIIGVTVV
Q9UEU0	Vesicle transport through interaction with t-SNAREs homolog 1B (Vesicle transport v-SNARE protein Vti1-like 1) (Vti1-rp1)	LSIIILLELAILGGLVYYKFF
A8MYB1	Transmembrane and coiled-coil domain-containing protein 5B	YFQYLTFMVLVFIRLLAYVIFHL
Q9BXK5	Bcl-2-like protein 13 (Bcl2-L-13) (Bcl-rambo) (Protein Mil1)	ILLFGGAAAVAILAVAIGVAL
Q6PJW8	Consortin	CILLVLLCIATVFLSVGGTAL
H3BV60	Transforming growth factor-beta receptor type 3-like protein (TGF-beta receptor type-3-like protein) (TGFR-3L) (Transforming growth factor-beta receptor type III-like protein) (TGF-beta receptor type III-like protein)	VVALVLAAFVLGAALAAGLGL
P17706	Tyrosine-protein phosphatase non-receptor type 2 (EC 3.1.3.48) (T-cell protein-tyrosine phosphatase) (TCPTP)	ILTKMGFMSVILVGAFVGWTLFF
Q8N111	Cell cycle exit and neuronal differentiation protein 1 (BM88 antigen)	LVAGGVAVAAIALILGVAFLV
E7ERA6	RING finger protein 223	LVSALLLMLFCVALWPVQCAL
O14653	Golgi SNAP receptor complex member 2 (27 kDa Golgi SNARE protein) (Membrin)	YFMIGGMLLTCVVMFLVVQYL

Supplemental Table 3. List of predicted human tail-anchored proteins (*continued*)

Entry	Protein names	TMD sequence
Q9BZ97	Putative transcript Y 13 protein	LLGWDLNLSLFLGLCLMLLLA
Q9P0L0	Vesicle-associated membrane protein-associated protein A (VAMP-A) (VAMP-associated protein A) (VAP-A) (33 kDa VAMP-associated protein) (VAP-33)	LPSLLVVIAAIFIGFFLGKFI
Q8N8J7	Uncharacterized protein C4orf32	VIVIFFWVMLWFLGLQALGLV
P37287	Phosphatidylinositol N-acetylglucosaminyltransferase subunit A (EC 2.4.1.198) (GlcNAc-PI synthesis protein) (Phosphatidylinositol-glycan biosynthesis class A protein) (PIG-A)	PVTGYIFALLAVFNFLFLIFL
Q5VV42	Threonylcarbamoyladenosine tRNA methylthiotransferase (EC 2.8.4.5) (CDK5 regulatory subunit-associated protein 1-like 1) (tRNA-t(6)A37 methylthiotransferase)	CALRMSVGLALLGLLFAFFVKVY
Q8WWG1	Pro-neuregulin-4, membrane-bound isoform (Pro-NRG4) [Cleaved into: Neuregulin-4 (NRG-4)]	EAFVALAVLVTLIIGAFYFLC
Q96NA8	t-SNARE domain-containing protein 1	CFLSAGVTALLVIIIIIATSV
Q68G75	LEM domain-containing protein 1 (Cancer/testis antigen 50) (CT50) (LEM domain protein 1) (LEMP-1)	FPVGLKLAVLGIFIIVVFVYL
P0CF51	T-cell receptor gamma chain C region 1	YYMYLLLLLKSVVYFAIITCCLL
Q9NX14	NADH dehydrogenase [ubiquinone] 1 beta subcomplex subunit 11, mitochondrial (Complex I-ESSS) (CI-ESSS) (NADH-ubiquinone oxidoreductase ESSS subunit) (Neuronal protein 17.3) (Np17.3) (p17.3)	LVFFFGVSIILVLGSTFVAYL
Q8IUY3	GRAM domain-containing protein 2A	LLKVFFVLICFLVMSSSYLAF
Q9UNK0	Syntaxin-8	MIMVILLLLVAIVVVAV
Q9GZT6	Coiled-coil domain-containing protein 90B, mitochondrial	TIRYLAASVFTCLAIALGFYRFW
O95249	Golgi SNAP receptor complex member 1 (28 kDa Golgi SNARE protein) (28 kDa cis-Golgi SNARE p28) (GOS-28)	SLILGGVIGICTILLLLYAFH
Q9P0B6	Coiled-coil domain-containing protein 167	MLLSVAIFILLTLVYAYW
Q9HDC5	Junctophilin-1 (JP-1) (Junctophilin type 1)	IMIVLVMLLNIGLAILFVHFL
Q8NF91	Nesprin-1 (Enaptin) (KASH domain-containing protein 1) (KASH1) (Myocyte nuclear envelope protein 1) (Myne-1) (Nuclear envelope spectrin repeat protein 1) (Synaptic nuclear envelope protein 1) (Syne-1)	AALPLQLLLLLLIGLACLVPM
Q8TBA6	Golgin subfamily A member 5 (Cell proliferation-inducing gene 31 protein) (Golgin-84) (Protein Ret-II) (RET-fused gene 5 protein)	VFVIIYMALLHLWVMIVLLTY
Q53EP0	Fibronectin type III domain-containing protein 3B (Factor for adipocyte differentiation 104) (HCV NS5A-binding protein 37)	IIVLGFATLSILFAFILQYFL
Q13323	Bcl-2-interacting killer (Apoptosis inducer NBK) (BIP1) (BP4)	VLLALLLLLALLLPLLSGGLH
Q9Y6F6	Protein MRVI1 (Inositol 1,4,5-trisphosphate receptor-associated cGMP kinase substrate) (JAW1-related protein MRVI1)	WQVIWMMAAVMLVLTVVLGLY
Q8N912	Nutritionally-regulated adipose and cardiac enriched protein homolog	GGSLLLQLCVCVLLVLALGLY
Q13948	Protein CASP	IGFFYTLFLHCLVFLVLYKLA
Q8WXI7	Mucin-16 (MUC-16) (Ovarian cancer-related tumor marker CA125) (CA-125) (Ovarian carcinoma antigen CA125)	FWAVILIGLAGLLGVITCLIC
Q14789	Golgin subfamily B member 1 (372 kDa Golgi complex-associated protein) (GCP372) (Giantin) (Macrogolgin)	VPLLAAIYFLMIHVLLILCFT
Q8WXH2	Junctophilin-3 (JP-3) (Junctophilin type 3) (Trinucleotide repeat-containing gene 22 protein)	LVVMVILLNIGVAILFINFFI
Q8TC41	Probable E3 ubiquitin-protein ligase RNF217 (EC 2.3.2.-) (IBR domain-containing protein 1) (RING finger protein 217)	LIMVLGLALGAIAVVIGLFVF

Supplemental Table 3. List of predicted human tail-anchored proteins (*continued*)

Entry	Protein names	TMD sequence
Q9Y6H6	Potassium voltage-gated channel subfamily E member 3 (MinK-related peptide 2) (Minimum potassium ion channel-related peptide 2) (Potassium channel subunit beta MiRP2)	YMYILFVMFLFAVTVGSLILG
Q8NCQ3	Putative uncharacterized protein encoded by LINC00301	SFGLAIIGILLIACEIILFLT
P0DN84	Sarcoplasmic/endoplasmic reticulum calcium ATPase regulator DWORF (SERCA regulator DWORF) (Dwarf open reading frame) (DWORF)	VPILLLIGWIVGCIIMIYVVF
P0DL12	Small integral membrane protein 17	IVLVVCVLFLFLVLTGMPMMF
Q86Z14	Beta-klotho (BKL) (BetaKlotho) (Klotho beta-like protein)	LIFLGCCFFSTLVLLLSIAIF
P59025	Receptor-transporting protein 1 (3CxxC-type zinc finger protein 1)	IPWCLFWATVLLLIIYLQFSF
Q5QGT7	Receptor-transporting protein 2 (3CxxC-type zinc finger protein 2)	LSLRWCLFWASLCLLVVYLQFSF
Q6ZS82	Regulator of G-protein signaling 9-binding protein (RGS9-anchoring protein)	ALAAILFGAVLLAAVALAVCV
Q9NYM9	BET1-like protein (Golgi SNARE with a size of 15 kDa) (GOS-15) (GS15) (Vesicle transport protein GOS15)	LLCGMAVGLIVAFFILSYFLS
Q9NRQ5	Single-pass membrane and coiled-coil domain-containing protein 4 (Protein FN5)	TVVLPTLAVVVLLIVVFVYVA
Q0VAQ4	Small cell adhesion glycoprotein (Small transmembrane and glycosylated protein)	IAVVITVVFLTLLSVVILIFF
Q96AG4	Leucine-rich repeat-containing protein 59 (Ribosome-binding protein p34) (p34) [Cleaved into: Leucine-rich repeat-containing protein 59, N-terminally processed]	WAVLKLLLLLLLFGVAGGLVA
Q9BR39	Junctophilin-2 (JP-2) (Junctophilin type 2)	ILICMVILLNIGLAILFVHLL
P23763	Vesicle-associated membrane protein 1 (VAMP-1) (Synaptobrevin-1)	MMIMLGAICAIIVVVIVIYF
Q96JN2	Coiled-coil domain-containing protein 136 (Nasopharyngeal carcinoma-associated gene 6 protein)	IFSLPLVGLVVISALLWCWWA
P51809	Vesicle-associated membrane protein 7 (VAMP-7) (Synaptobrevin-like protein 1) (Tetanus-insensitive VAMP) (Ti-VAMP)	LTIIIIIVSIVFIYIIVSPLC
Q9BQQ7	Receptor-transporting protein 3 (3CxxC-type zinc finger protein 3) (Transmembrane protein 7)	SIFCCCVILIVIVVIVVKTAI
O00631	Sarcolipin	LFLNFTIVLITVILMWLLV
A6NCQ9	RING finger protein 222	LITLIAVVAVVAAILPWVLLV
Q8WWP7	GTPase IMAP family member 1 (Immunity-associated protein 1) (hIMAP1)	SWRLGLALLLGGALLFWVLL
Q96D05	Uncharacterized protein C10orf35	ILLLFLLMMLGVRGLLLVGLV
Q9Y2H6	Fibronectin type-III domain-containing protein 3A (Human gene expressed in odontoblasts)	ILVLFAFFSILIAFIIQYFVI
P04921	Glycophorin-C (Glycoconnectin) (Glycophorin-D) (GPD) (Glycoprotein beta) (PAS-2') (Sialoglycoprotein D) (CD antigen CD236)	DIVVIAGVIAAVAIVLVSLLFVML
Q8N8N0	E3 ubiquitin-protein ligase RNF152 (EC 2.3.2.27) (RING finger protein 152) (RING-type E3 ubiquitin transferase RNF152)	SGVCTVILVACVLVFLLGIVL
A6NNC1	Putative POM121-like protein 1-like	LGLFLLVFSFFFLLTWASFSF
Q12912	Lymphoid-restricted membrane protein (Protein Jaw1) [Cleaved into: Processed lymphoid-restricted membrane protein]	ALWLSIAFIVLFAALMSFLTG
P61566	Endogenous retrovirus group K member 24 Env polyprotein (Envelope polyprotein) (HERV-K101 envelope protein) (HERV-K_22q11.21 provirus ancestral Env polyprotein) [Cleaved into: Surface protein (SU); Transmembrane protein (TM)]	IGSTTIINLILILVCLFCLLL
P61567	Endogenous retrovirus group K member 7 Env polyprotein (Envelope polyprotein) (HERV-K(III) envelope protein) (HERV-K102 envelope protein) (HERV-K_1q22 provirus ancestral Env polyprotein) [Cleaved into: Surface protein (SU); Transmembrane protein (TM)]	IGSTTIINLILILVCLFCLLL
Q8N6L0	Protein KASH5 (Coiled-coil domain-containing protein 155) (KASH domain-containing protein 5)	LIPAPVLGLLLLLLLSVLLLG

Supplemental Table 3. List of predicted human tail-anchored proteins (*continued*)

Entry	Protein names	TMD sequence
Q8N6Q1	Transmembrane and coiled-coil domain-containing protein 5A	IFCCLFFITLFFIRLLSYMFF
Q12981	Vesicle transport protein SEC20 (BCL2/adenovirus E1B 19 kDa protein-interacting protein 1) (Transformation-related gene 8 protein) (TRG-8)	TDKLLIFLALALFLATVLYIV
P59773	UPF0258 protein KIAA1024-like	GLILLVVISILVTIVTIITFF
Q8WXH0	Nesprin-2 (KASH domain-containing protein 2) (KASH2) (Nuclear envelope spectrin repeat protein 2) (Nucleus and actin connecting element protein) (Protein NUANCE) (Synaptic nuclear envelope protein 2) (Syne-2)	AALPLQLLLLLLLLLACLLPS
Q8WVX3	Uncharacterized protein C4orf3 (Hepatitis C virus F protein-transactivated protein 1) (HCV F-transactivated protein 1)	WLDLWLFILFDVVVFLFVYFL
P32856	Syntaxin-2 (Epimorphin)	WIIIAVSVVLVAIIALIIGLSVGK
Q6IEE8	Schlafen family member 12-like	IFLFVCLFRFCLFVCWFVCFF
Q8NHP6	Motile sperm domain-containing protein 2	LLLSLTMLLLAFVTSFFYLLY
O95292	Vesicle-associated membrane protein-associated protein B/C (VAMP-B/VAMP-C) (VAMP-associated protein B/C) (VAP-B/VAP-C)	RLLALVVLFFIVGVIIGKIAL
Q96QK8	Small integral membrane protein 14	GISVTMILVAWMVIALILFLL
Q96JQ2	Calmin (Calponin-like transmembrane domain protein)	MMYFILFLWLLVYCLLLFPQL
Q71RC9	Small integral membrane protein 5	IVAFSVIILFTATVLLLLLIA
A2A2Y4	FERM domain-containing protein 3 (Band 4.1-like protein 4O) (Ovary type protein 4.1) (4.1O)	LLVVGLGLLLFVFPLLLLLLE
O42043	Endogenous retrovirus group K member 18 Env polyprotein (Envelope polyprotein) (HERV-K(C1a) envelope protein) (HERV-K110 envelope protein) (HERV-K18 envelope protein) (HERV-K18 superantigen) (HERV-K_1q23.3 provirus ancestral Env polyprotein) (IDDMK1,2 22 envelope protein) (IDDMK1,2 22 superantigen) [Cleaved into: Surface protein (SU); Transmembrane protein (TM)]	IRSTMIINLILIVVCLFCLLL
P50402	Emerin	VPLWGQLLLFLVFVIVLFFIY
Q96D59	Probable E3 ubiquitin-protein ligase RNF183 (EC 2.3.2.27)	IFAYLMAVILSVTLLLIFSIF
Q9P2W9	Syntaxin-18 (Cell growth-inhibiting gene 9 protein)	AGFRVWILFFLVMCSFSLLFL
Q01629	Interferon-induced transmembrane protein 2 (Dispanin subfamily A member 2c) (DSPA2c) (Interferon-inducible protein 1-8D)	IWALILGIFMTILLIIIPVLV
Q86Y82	Syntaxin-12	KKMCILVLVLSVIILILGLII
Q01628	Interferon-induced transmembrane protein 3 (Dispanin subfamily A member 2b) (DSPA2b) (Interferon-inducible protein 1-8U)	IWALILGILMTILLIVIPVLI
P0C2S0	Cortexin-2	TGFAFVGILCIFLGLLIIRCF
O75396	Vesicle-trafficking protein SEC22b (ER-Golgi SNARE of 24 kDa) (ERS-24) (ERS24) (SEC22 vesicle-trafficking protein homolog B) (SEC22 vesicle-trafficking protein-like 1)	KLAAVAVFFIMLIVYVRFWWL
P42167	Lamina-associated polypeptide 2, isoforms beta/gamma (Thymopoietin, isoforms beta/gamma) (TP beta/gamma) (Thymopoietin-related peptide isoforms beta/gamma) (TPRP isoforms beta/gamma) [Cleaved into: Thymopoietin (TP) (Splenin); Thymopentin (TP5)]	IPVWIKILLFVVVAVFLFLVYQAM
P13164	Interferon-induced transmembrane protein 1 (Dispanin subfamily A member 2a) (DSPA2a) (Interferon-induced protein 17) (Interferon-inducible protein 9-27) (Leu-13 antigen) (CD antigen CD225)	IWALILGILMTIGFILLLVFG
Q0VDE8	Adipogenin	FSFLVFWFCLPVGLLLLLIIW
Q9BZL3	Small integral membrane protein 3 (NGF-induced differentiation clone 67 protein) (Small membrane protein NID67)	IWVIVLIILATIVIMTSLLLC

Supplemental Table 3. List of predicted human tail-anchored proteins (*continued*)

Entry	Protein names	TMD sequence
Q96AJ9	Vesicle transport through interaction with t-SNAREs homolog 1A (Vesicle transport v-SNARE protein Vti1-like 2) (Vti1-rp2)	ILLVILGIIVVITILMAITFS
O75379	Vesicle-associated membrane protein 4 (VAMP-4)	IKAIMALVAAILLLVIIILIV
O95159	Zinc finger protein-like 1 (Zinc finger protein MCG4)	LLLLLGLLGFLALLALMSRLG
Q86Y07	Serine/threonine-protein kinase VRK2 (EC 2.7.11.1) (Vaccinia-related kinase 2)	VYYYRIIIPVLLMLVFLALFF
Q86W74	Ankyrin repeat domain-containing protein 46 (Ankyrin repeat small protein) (ANK-S)	LGFWRVLLLIFVIALLSLGIA
Q629K1	Triple QxxK/R motif-containing protein (Triple repetitive-sequence of QXXK/R protein homolog)	VGLVLAAILALLLAFYAFFYL
P0DKX4	Small integral membrane protein 18	CFVILLLFIFTVVSLVVLAFL
Q8N8F7	Leucine-rich single-pass membrane protein 1	VGLLIVLIVSLALVFFVIFLI
O15155	BET1 homolog (hBET1) (Golgi vesicular membrane-trafficking protein p18)	KLLCYMMLFSLFVFFIIYWII
P63027	Vesicle-associated membrane protein 2 (VAMP-2) (Synaptobrevin-2)	MMIILGVICAIILIIIIVYF
O15400	Syntaxin-7	CIIILILVIGVAIISLIIWGL
A2A2V5	Serine-rich and transmembrane domain-containing protein 1	IYVSIFLSLLAFLLLLLIIAL
Q6ZMZ3	Nesprin-3 (KASH domain-containing protein 3) (KASH3) (Nuclear envelope spectrin repeat protein 3)	VALPLQLLLLLFLLLLFLLPI
O60499	Syntaxin-10 (Syn10)	WCAIAVLVGVLLLVLILLFSL
P60606	Cortexin-1	TVFAFVLCLLVVLVLLMVRCV
Q13277	Syntaxin-3	LIIIIVLVVVLLGILALIIGL
O95183	Vesicle-associated membrane protein 5 (VAMP-5) (Myobrevin)	VGLVVVGVLLIILIVLLVVFL
Q7Z6J6	FERM domain-containing protein 5	LLLVTMGLLFVLLLLLIILTE
Q15836	Vesicle-associated membrane protein 3 (VAMP-3) (Cellubrevin) (CEB) (Synaptobrevin-3)	MWAIGITVLVIFIIIIIVWVV
Q4LDR2	Cortexin-3 (Kidney and brain-expressed protein)	MTFVFVILLFIFLGILIVRCF
A9Z1Z3	Fer-1-like protein 4	LVLLLLVLLTVFLLLVFYTIP
Q9HCU5	Prolactin regulatory element-binding protein (Mammalian guanine nucleotide exchange factor mSec12)	VPVWLLLLLCVGLIIVTILLL
Q8N112	Leucine-rich single-pass membrane protein 2	GFLLLLALLVLTCLVLALLAV
Q13190	Syntaxin-5	WLMVKIFLILIVFFIIFVVFL
P0DI80	Small integral membrane protein 6	LAVIILFITAVLLLILFAIVF
Q96F15	GTPase IMAP family member 5 (Immunity-associated nucleotide 4-like 1 protein) (Immunity-associated nucleotide 5 protein) (IAN-5) (hIAN5) (Immunity-associated protein 3)	IFVFLLLCSILFFIIFLFIFH
Q9NX77	Endogenous retrovirus group K member 13-1 Env polyprotein (Envelope polyprotein) (HERV-K_16p13.3 provirus ancestral Env polyprotein) [Cleaved into: Surface protein (SU); Transmembrane protein (TM)]	GSLLLLALLILVCLCCLLLVC
Q8N205	Nesprin-4 (KASH domain-containing protein 4) (KASH4) (Nuclear envelope spectrin repeat protein 4)	FLLILFLLFLLLVGAMFLLPA
P26678	Cardiac phospholamban (PLB)	FINFCLILICLLLICIIVMLL
O14662	Syntaxin-16 (Syn16)	MLVILILFVIIIVLIVVLVGV

Supplemental Table 3. List of predicted human tail-anchored proteins (*continued*)

Entry	Protein names	TMD sequence
Q9BV40	Vesicle-associated membrane protein 8 (VAMP-8) (Endobrevin) (EDB)	MIVLICVIVFIIILFIVLFAT
Q9NZ43	Vesicle transport protein USE1 (Putative MAPK-activating protein PM26) (USE1-like protein) (p31)	WLLWAMLIIVCFIFISMILFI
O43752	Syntaxin-6	WCAIAILFAVLLVVLILFLVL
Q9NZM1	Myoferlin (Fer-1-like protein 3)	WVIIGLLFLLILLLFVAVLLY
O75923	Dysferlin (Dystrophy-associated fer-1-like protein) (Fer-1-like protein 1)	IILFIILFILLLFLAIFIYAF
Q2WGJ9	Fer-1-like protein 6	IIIAFILIILIIFLVLFIYTL
Q9HC10	Otoferlin (Fer-1-like protein 2)	WLLLKLLLLLLLLLLLALFLY

TMD, transmembrane domain.

Supplemental Table 4. Animal models for ASNA1-mediated TA protein insertion related genes

Gene	Synonyms	Species	Genotype	Mechanism	Phenotype	Refs
WRB	*CHD5, GET1*	*Mus musculus*	$Wrb^{tm1.1(KOMP)Vlcg}/Wrb^{tm1.1(KOMP)Vlcg}$	homozygous ko	embryonic lethality (<E9.5)	6
		Mus musculus	$Wrb^{tm1.1(KOMP)Vlcg}/Wrb+$	heterozygous ko	abnormal brain development	6
		Mus musculus	$Wrb^{fl/fl}$:Vglut3-Cre $Wrb^{fl/fl}$:Vglut3-ires-Cre	conditional ko	progressive hearing impairment, tonic-clonic seizures	7
		Danio rerio	$wrb^{hi1482Tg}$	homozygous ko	abnormal myocardial repolarization, bradycardia	8
		Danio rerio	$wrb^{hi1482Tg/hi1482Tg}$ $wrb^{hi1482Tg/hi1482Tg}$; nl1Tg	homozygous ko	reduced auditory startle response, reduced visual evoked potentials	9
		Danio rerio	lri48Tg ; $wrb^{hi1482Tg}$ q16aTg ; q16bTg ; $wrb^{hi1482Tg/hi1482Tg}$ $wrb^{hi1482Tg/hi1482Tg}$	homozygous ko	photoreceptor synapse defects	10
		Danio rerio	$wrb^{hi1482Tg/hi1482Tg}$	homozygous ko	impaired hair cell exocytosis and hearing	7
		Oryzias latipalis	WT + MO chd5 (ATG)	knockdown	cardiac looping defects, abnormal chamber differentiation, ocular abnormalities	11
		Xenopus tropicalis	$Tg(actc1:GFP)^{Mohun}$ + MO chd5 (ATG) $Tg(actc1:GFP)^{Mohun}$ + MO chd5 (SB)	knockdown	cardiac looping defects, abnormal chamber differentiation	12
CAMLG	*CAML, GET2*	*Mus musculus*	$Caml^{tm1Rjb}/Caml^{tm1Rjb}$	homozygous ko	embryonic lethality (E4.5-E7.5)	13
		Mus musculus	$Caml^{tm1Rjb}/Caml^{tm2Rjb}$	conditional ko	abnormal T-cell development	14
ASNA1	*TRC40, GET3*	*Mus musculus*	$Asna1^{tm1Hbha}/Asna1^{tm1Hbha}$	homozygous ko	embryonic lethality (E3.5-E8.5)	15
		Danio rerio	q16aTg ; q16bTg + MO1 asna1 WT + MO1 asna1 (ATG) WT + MO2 asna1 (SB)	knockdown	decreased visual perception, photoreceptor synapse defects, lack of swim bladder	10
		Danio rerio	$asna1^{\Delta 7/\Delta 7}$	homozygous ko	impaired swim bladder inflation, decreased blood flow in dorsal aorta, impaired cardiac contractility, early lethality (6-8 dpf)	This study

ATG, translation-blocking; dpf, days post fertilization; E, embryonic day; ko, knock-out; MO, morpholino; SB, splice-blocking; WT, wild-type.

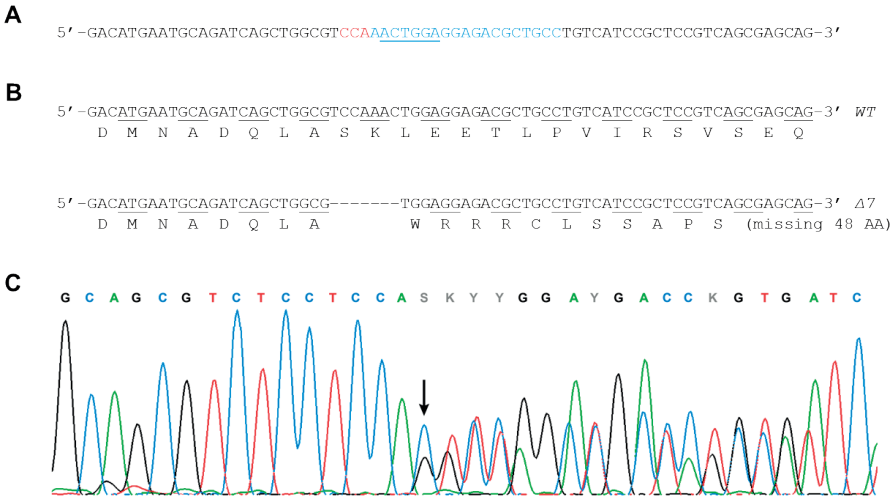

Supplemental Figure 1. CRISPR/Cas9-induced *asna1* deletion in zebrafish. (A) Schematic representation of guide RNA target site (*asna1* exon 5). Protospacer is highlighted in blue; PAM in red. BsrI recognition site used for genotyping is underlined. (B) Sequence and position of induced 7 bp deletion (Δ7) predicted to result in a frameshift and premature stop codon. (C) Chromatogram of PCR-amplified DNA from F1 fish showing wild-type and mutant sequence (reverse complement). The arrow indicates the position of the deletion.

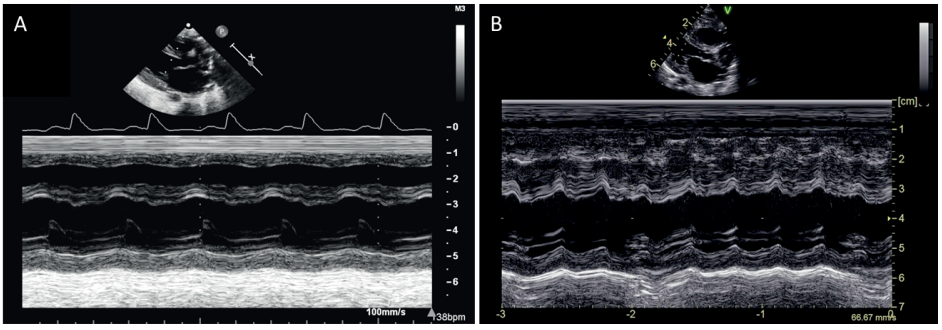

Supplemental Figure 2. M-mode imaging in both patients. M-mode image of the heart in parasternal long axis view in (top) patient II:2 and (B) patient II:3 showing severly reduced left ventricular contractility.

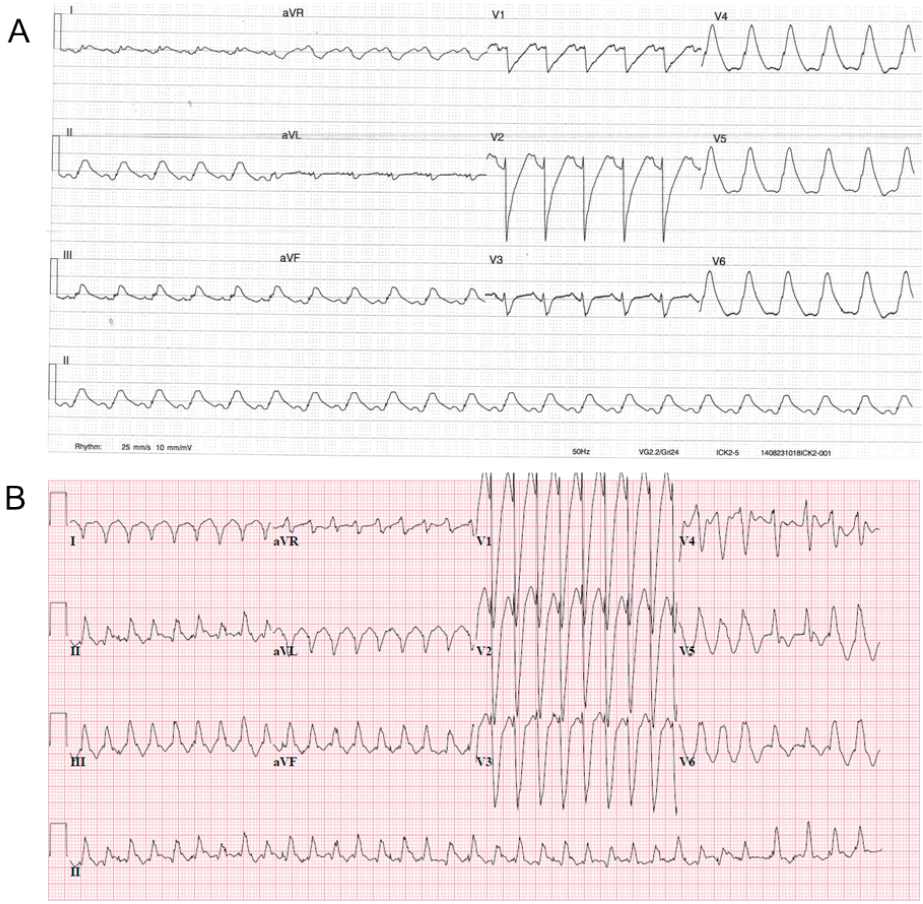

Supplemental Figure 3. Electrocardiography recordings of both patients. (A) ECG of patient II:2 during hospital admission showing sinus rhythm at a rate of 130/min with extremely broad QRS complexes of 220 ms and normal QRS axis of 60 degrees. (B) ECG of patient II:3 during cardiopulmonary resuscitation (no prior ECG available).

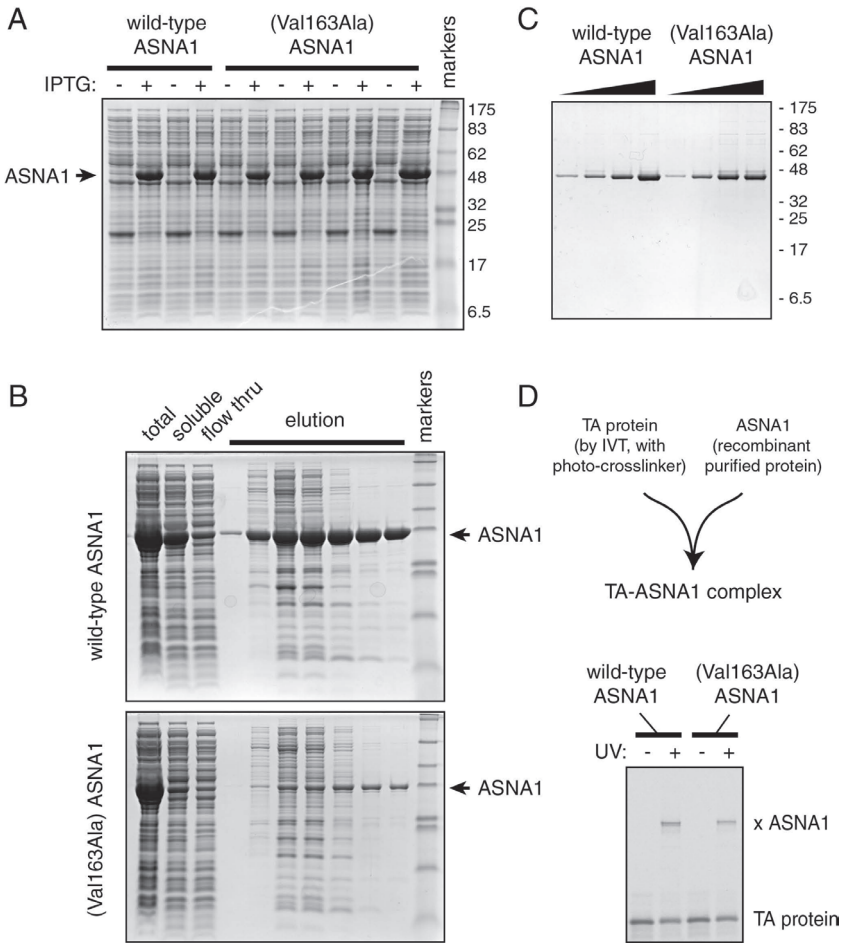

Supplemental Figure 4. Recombinant expression and purification of ASNA1 from *E. coli*. (A) Expression tests of *E. coli* transformed with plasmids encoding either wild-type ASNA1 or the Val163Ala mutant. In each case, equal numbers of cells harvested before or after induction with 1 mM IPTG (for 3 hours at 37°C) were analyzed by SDS-PAGE and staining with Coomassie Blue. Two individual isolates of wild-type and four of mutant ASNA1 all show comparable expression levels of recombinant ASNA1 (indicated by the arrow). (B) The cells from a larger scale induction of wild-type and mutant ASNA1 (as in panel A) were collected, lysed by sonication, and subjected to chromatography using Ni-NTA columns. The total cells, soluble lysate, flow through, and elution fractions are shown. Note that a substantially higher proportion of wild-type ASNA1 is produced as a soluble protein, and recovered by chromatography. This is a consistent effect observed in more than six independent trials. (C) Increasing amounts of purified wild-type or mutant ASNA1 (ranging from 100 ng to 1 µg protein) were analyzed by SDS-PAGE and Coomassie staining to document concentration and purity. (D) A model TA protein containing the transmembrane domain from VAMP2 was translated in a purified *E. coli*-based translation system [16]. This system contains only recombinant translation factors and ribosomes, with no additional proteins. In addition, it contains ^{35}S-methionine to label the newly synthesized TA protein, and the photo-crosslinking amino acid benzyl-phenylalanine (BPA) and components for its incorporation at amber codons. A single amber codon in the transmembrane domain of the TA protein is used to incorporate this photo-crosslinking amino acid. The translation was supplemented with either wild-type or mutant ASNA1, which forms a complex with the newly made TA protein. The successful formation of the TA-ASNA1 complex was verified by UV irradiation to induce a covalent crosslink between these two proteins (indicated by "x ASNA1"). These recombinant TA-ASNA1 complexes were used for the insertion assay shown in Figure 4D.

Supplemental References

1. Shao S, Rodrigo-Brenni MC, Kivlen MH, Hegde RS. Mechanistic basis for a molecular triage reaction. *Science.* 2017;355:298-302.
2. Guna A, Volkmar N, Christianson JC, Hegde RS. The ER membrane protein complex is a transmembrane domain insertase. *Science.* 2018;359:470-473.
3. Westerfield M. *The zebrafish book. A guide for the laboratory use of zebrafish (Danio rerio).* 4th Edition ed. Eugene, OR: University of Oregon Press; 2000.
4. D'Astolfo DS, Pagliero RJ, Pras A, Karthaus WR, Clevers H, Prasad V, et al. Efficient intracellular delivery of native proteins. *Cell.* 2015;161:674-690.
5. Brinkman EK, Chen T, Amendola M, van Steensel B. Easy quantitative assessment of genome editing by sequence trace decomposition. *Nucleic Acids Res.* 2014;42:e168.
6. Blake JA, Eppig JT, Kadin JA, Richardson JE, Smith CL, Bult CJ, et al. Mouse Genome Database (MGD)-2017: community knowledge resource for the laboratory mouse. *Nucleic Acids Res.* 2017;45:D723-D729.
7. Vogl C, Panou I, Yamanbaeva G, Wichmann C, Mangosing SJ, Vilardi F, et al. Tryptophan-rich basic protein (WRB) mediates insertion of the tail-anchored protein otoferlin and is required for hair cell exocytosis and hearing. *Embo J.* 2016;35:2536-2552.
8. Milan DJ, Kim AM, Winterfield JR, Jones IL, Pfeufer A, Sanna S, et al. Drug-sensitized zebrafish screen identifies multiple genes, including GINS3, as regulators of myocardial repolarization. *Circulation.* 2009; 120:553-559.
9. Lin SY, Vollrath MA, Mangosing S, Shen J, Cardenas E, Corey DP. The zebrafish pinball wizard gene encodes WRB, a tail-anchored-protein receptor essential for inner-ear hair cells and retinal photoreceptors. *J Physiol.* 2016;594:895-914.
10. Daniele LL, Emran F, Lobo GP, Gaivin RJ, Perkins BD. Mutation of wrb, a Component of the Guided Entry of Tail-Anchored Protein Pathway, Disrupts Photoreceptor Synapse Structure and Function. *Invest Ophthalmol Vis Sci.* 2016;57:2942-2954.
11. Murata K, Degmetich S, Kinoshita M, Shimada E. Expression of the congenital heart disease 5/tryptophan rich basic protein homologue gene during heart development in medaka fish, Oryzias latipes. *Dev Growth Differ.* 2009;51:95-107.
12. Sojka S, Amin NM, Gibbs D, Christine KS, Charpentier MS, Conlon FL. Congenital heart disease protein 5 associates with CASZ1 to maintain myocardial tissue integrity. *Development.* 2014;141:3040-3049.
13. Tran DD, Russell HR, Sutor SL, van Deursen J, Bram RJ. CAML is required for efficient EGF receptor recycling. *Dev Cell.* 2003;5:245-256.
14. Tran DD, Edgar CE, Heckman KL, Sutor SL, Huntoon CJ, van Deursen J, et al. CAML is a p56Lck-interacting protein that is required for thymocyte development. *Immunity.* 2005;23:139-152.
15. Mukhopadhyay R, Ho YS, Swiatek PJ, Rosen BP, Bhattacharjee H. Targeted disruption of the mouse Asna1 gene results in embryonic lethality. *FEBS Lett.* 2006;580:3889-3894.
16. Shimizu Y, Ueda T. PURE technology. *Methods Mol Biol.* 2010;607:11-21.